PHYSICAL OCEANOGRAPHIC MEASUREMENTS IN THE NORTHEASTERHN CHUKCHI SEA: 2011

Prepared for

ConocoPhillips, Inc.
P.O. Box 100360
Anchorage, AK 99510-0360

Shell Exploration & Production Company
3601 C Street, Suite 1334
Anchorage, AK 99503

and

Statoil USA E&P, Inc.
2700 Gambell Street
Anchorage, AK 99507

FINAL REPORT

Prepared by

Thomas Weingartner, Seth Danielson, Liz Dobbins, and Rachel Potter

Institute of Marine Science
University of Alaska
Fairbanks, AK 99775

December 2012

Introduction

This report provides a partial synopsis of the data set collected in summer 2011 from the northeastern Chukchi Sea in areas potentially subject to and influenced by offshore oil exploration activities. Prior years' data and interpretations were summarized in previous reports and most recently by the synthesis of Weingartner et al. (*in review*) and will not be repeated in detail herein.

As noted previously seasonal changes in Chukchi Sea water properties are established by the annual cycles of sea-ice formation and ablation, air-sea heating/cooling and wind mixing, and transport of waters from Bering Strait. In summer and early fall, the Strait transport is northward on average and includes three major water masses, which following the nomenclature of Coachman et al. (1975) and Walsh et al. (1989) are: cold, salty, nutrient-rich Anadyr Water; warm, fresh, nutrient-poor Alaskan Coastal Water (ACW); and Bering Shelf Water. The latter has properties intermediate between, but nonetheless distinct from, the Anadyr and Alaskan Coastal water masses. Coachman et al. (1975) maintain that the Anadyr and Bering Shelf water masses mix to form Bering Sea Water (BSW) north of the Strait, whereas ACW maintains its properties on the Chukchi shelf. In summer and fall, Chukchi bottom waters often include near-freezing, saline (dense) waters that formed in winter by freezing over both the Bering and Chukchi seas. In addition, shallow plumes of cool, dilute, surface waters, formed by ice melt, may also be present.

Figure 1 illustrates the mean circulation over the shelf based on the model of Spall (2007), which largely agrees with the inferences drawn from the observations. Although the mean flow is nominally northward over much of the shelf, the bulk of the transport proceeds along three principal pathways with each pathway associated with a distinct bathymetric feature; Herald Canyon, the Central Channel, and Barrow Canyon. The troughs are separated from one another by shoals: Herald Shoal separates Herald Canyon from the Central Channel and Hanna Shoal lies between Barrow Canyon and the Central Channel.

BSW is transported to the northwest Chukchi, over the central shelf, and northward through the Central Channel (Fig. 1a; Weingartner et al., 2005; Woodgate et al., 2005). Weingartner et al. (2005) suggested that, south of Hanna Shoal, some central-shelf waters flow eastward toward the coast, in agreement with the circulation models of Winsor and Chapman (2004) and Spall (2008). North of the Central Channel, where there are no long-term current measurements, both models suggest the average flow follows the bathymetry around the western and northern flanks of Hanna Shoal before turning southward along the eastern side of the Shoal before eventually entering Barrow Canyon. However, the models also predict that some of the water along the eastern flank of Hanna Shoal penetrates southwestward along the southern flank of the Shoal before turning eastward towards the coast. The ACW flows northeastward within the Alaskan Coastal Current toward the head of Barrow Canyon. Here it merges with waters flowing eastward from the central shelf to form the canyon outflow. Hence in summer and fall, the canyon outflow contains a horizontally- and vertically-structured complex of water masses (Pickart et al., 2005; Shroyer and Plueddemann, 2012) that include ACW, meltwater, dense winter waters, BSW, and mixtures of each.

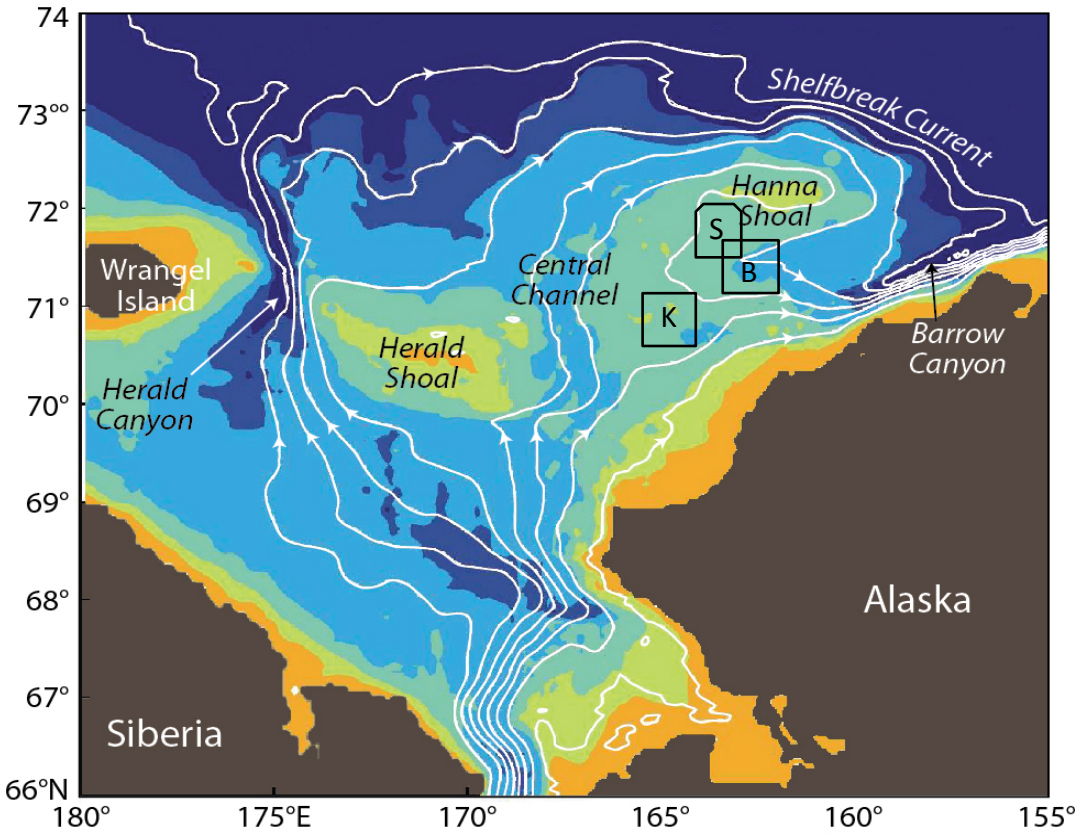

Figure 1. Mean depth-integrated streamlines (white lines) in the Chukchi Sea, after Spall, (2007). The bathymetry is colored and major bathymetric features are labeled. The lettered boxes denote the approximate locations of the Klondike (K), Burger (B), and Statoil (S) survey areas.

Two further aspects of the circulation depicted in Figure 1 deserve further emphasis. First, note the streamline intersecting the Statoil survey area. The model results indicate that the flow here is southward through Statoil before veering eastward along the northern edge of the Klondike survey area. Weingartner et al. (*in review*) suggest that the flow across Statoil is southeastward at least over the western half of Statoil, with this flow then merging with an eastward flow emanating from Klondike. It appears that these flows converge along the southern half of Burger. Second, the acute curvature of the streamline in Burger implies that water is being carried from the eastern side of Hanna Shoal into Burger before turning eastward toward the coast. That water includes meltwater in the upper water column and dense, winter water in the lower portion of the water column. Weingartner et al., (in review) infer that this model prediction is correct, at least intermittently. The implications of these findings are that in summer BSW is flows eastward from the Central Channel across both Klondike and the western half of Statoil. This flow then converges with the waters entering Burger from the northeast. Eventually all of these water masses flow eastward and enter Barrow Canyon. The conclusions of Weingartner et al. (in review), are further supported by the data collected in summer 2011 and discussed below.

Methods

The sampling discussed in this report was in the northeast Chukchi Sea and included repeated surveys in the Klondike, Burger and Statoil study areas (**Figure 2**) and over a much broader region surrounding these areas (**Figure 2**). Note that the Klondike study area lies to the east of

the Central Channel, whereas Statoil is along the southwest flank of Hanna Shoal and Burger is on the southern flank of this shoal. Water depths in the region are ~40 – 45 m.

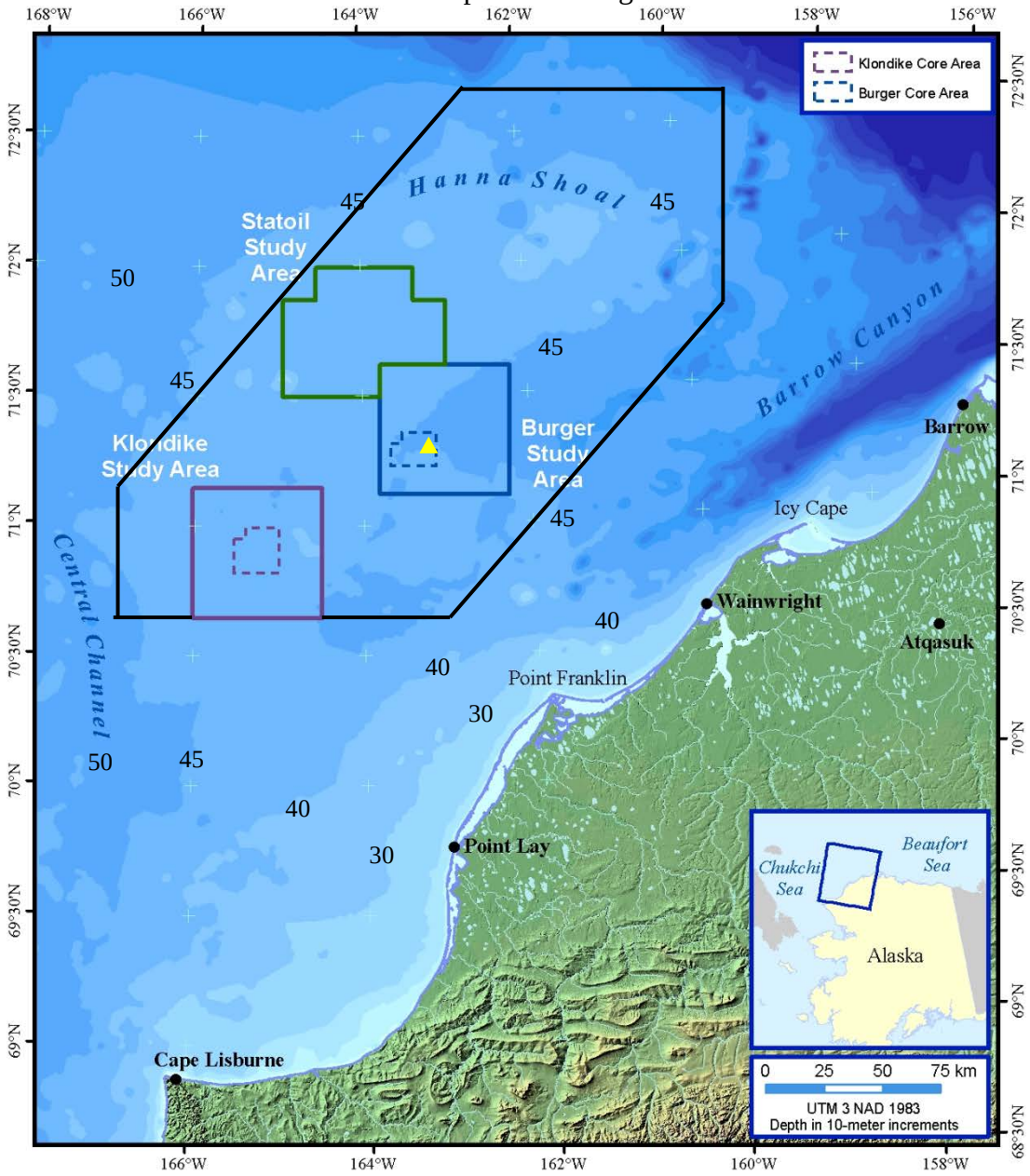

Figure 2. Map showing locations of the Klondike, Burger, and Statoil study areas in relation to the Alaskan coast. The yellow triangle shows the approximate location of the NCEP-NARR meteorological grid point used to assess the regional winds. The black line encompasses the sampling conducted within the regional survey between 31 August and 4 October 2011.

Data were collected with a Seabird, Inc. SBE-19+V2 CTD sampling at 4 Hz. The instrument was lowered throughout the water column at a rate of ~0.5m min^{-1} so that ~480 samples m^{-1} were obtained. Measured variables include pressure, temperature, conductivity, beam attenuation, beam transmission, and fluorescence. Derived variables include depth, salinity, density and speed of sound. The data were processed according to the manufacturer's recommended

procedures [provided in the SBE Data Processing manual) and further screened for anomalous spikes, dropouts and density inversions. Data are averaged to 1 decibar (approximately 1 meter) vertical profiles. Post-season calibrations of the temperature and conductivity cells are performed at the manufacturer's calibration facility. Comparison of the pre- and post-calibration values indicate that the temperature data are accurate to better than 0.005 °C and salinity to 0.02.

The stations occupied during the two CTD cruises are shown in Figure 3, with the color shading indicating the Julian day of the sampling. During the 6 23 August survey sampling began at Klondike, then moved to Burger, before ending at the northernmost end of Statoil. The broad-scale survey commenced on August 31 at the southern end of the study region and then proceeded westward across Klondike. Thereafter sampling included proceeded across a portion of Burger, thence Statoil, and the remainder of Burger. Once Burger was completed the stations over and north of Hanna Shoal were occupied. Stations along the northeasternmost side of the broader region were occupied at the end of the cruise. We present these sampling times to emphasize that the results cannot be considered synoptic, except within Klondike, Burger, and Statoil, given the time differences in the sampling. This holds especially for the second cruise, in which the last station was occupied 35 days after the first station. The results presented below are likely aliased because of the lack of synopticity and thus our interpretation should be viewed with this caveat.

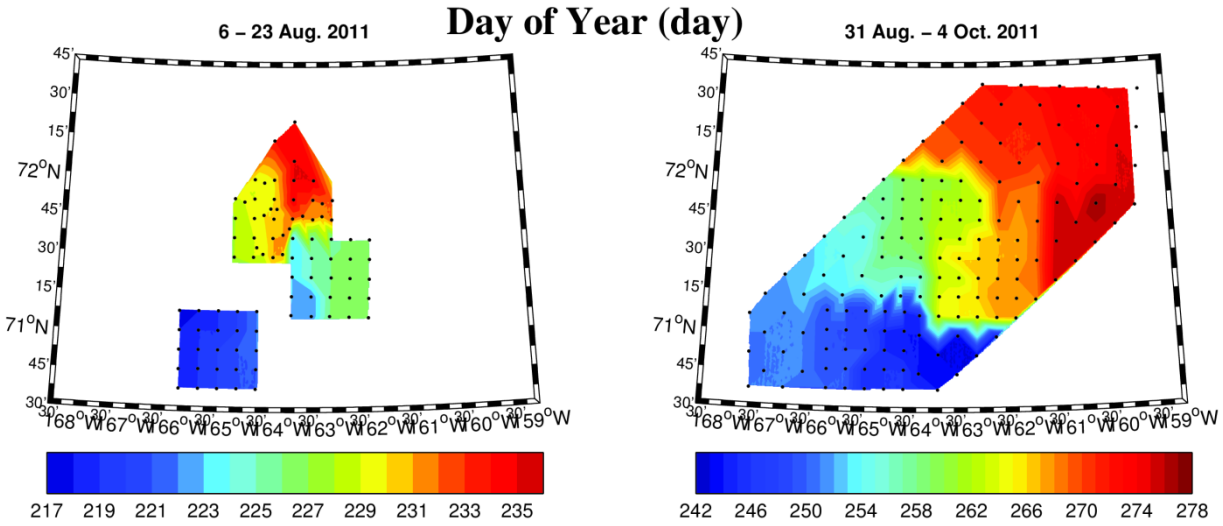

Figure 3. Contours showing the Julian day of year of CTD station occupations during the 2011 cruises.

Winds

We used 3-hourly winds produced by the National Center for Environmental Prediction North American Regional Re-analysis (NARR) model hindcasts (Mesinger et al., 2006).

ADCP data quality and processing summary:

A 600-KHz Teledyne-RDI acoustic Doppler current profiler (ADCP) was operated during the 2010 Chukchi field season. Setup, operating parameters, transformations and error-screening procedures are listed in the **Tables 1** and **2**. Initial data screenings were performed in the TRDI

software package VmDAS. Final data assessment and transformations were made in the MATLAB programming language with custom software. Data QA/QC parameters are listed in **Table 3**. After evaluating each 1-minute ensemble, consisting of 60 1-second pings, the data were averaged into 6-hour bins and plotted. **Figures 4 and 5** show the temporal distribution of the 6-hourly averaged ensembles for the 4 August to 3 October period. In order to form a 6-hour average at least 25% of the ensembles collected during that 6-hour period had to have had good data. Time series of the percent good, error and vertical velocity time series as a function of depth and 6-hour averaged ensemble are shown in **Figures 6 and 7**. Inspection of these data suggested that the first depth bin which yielded reliably acceptable data was 11 – 15 m below the surface. Velocities were also depth-averaged into 2-m deep bins.

Table 1. ADCP Setup and Navigation parameters.

System	Teledyne RDI Workhorse
Frequency	600KHz
Installation	Vessel-attached pole-mount
Orientation	Downward
Operating mode	Broadband
Bottom Track	Yes
Time per ping	1 s
Number of bins:	25
Bin size	2 m
Blanking Distance	2 m
Transducer Depth	3m
Ship position	NMEA1 GGA
Ship speed	NMEA2 VTG
Tilt source	ADCP internal tilt sensor
Heading source:	NMEA2 HDT
Alignment Error:	40.38^{o}

Overall data quality was good, although there were periods with poor data (**Figures 4 - 7**) that corresponded to rough seas. This can result in loss of bottom-tracking and/or bubble entrainment below the transducer. Vessel speed and orientation with respect to direction of the surface wave field may also impact data quality. In general, data quality decreases if the vessel is heading into heavy seas. Again, the interpretation of these data is hampered by the absence of synopticity and thus remain an ongoing exercise. However, we do show results of the vessel-mounted ADCP survey conducted between 28 July and 3 August 2011, in which the velocity field can be regarded as synoptic.

Table 2. VmDAS averaging and data screening thresholds.

STA average interval	60s
Profile Ping Normalization reference layer	Bins 3 - 10
Water Current Profile Received Signal Strength Indicator	80 counts
Water Current Profile Correlation	180 counts
Water Current Profile Error Velocity	1 m/s
Water Current Profile Vertical Velocity	1 m/s
Water Current Profile Fish target	50 counts
Water Current Profile Percent Good	50%
Bottom Track Received Signal Strength Indicator	30 counts
Bottom Track Correlation	220 counts
Bottom Track Error Velocity	1 m/s
Bottom Track Fish:	50 counts
Bottom Track Vertical Velocity	1 m/s
Bottom Track Percent Good	50%

Table 3. QA/QC thresholds and corrections applied to 1-minute STA ensembles.

Minimum correlation	64
Minimum percent-good 4-beam + 3-beam solutions	50%
Minimum percent-good bottom track pings	25%
Blanking above bottom (% of distance to transducer)	6%
Maximum heading standard deviation	3
Maximum change in speed	0.2 m/s
Minimum speed	1.5 m/s
Maximum vertical velocity	0.1 m/s
Maximum error velocity	0.05 m/s
Minimum good fraction of water profile allowed	2/3
Individual ensemble cross-track magnitude/direction corrections	Yes
Transducer mis-alignment correction	-0.49°
Ensembles removed with unrealistically large mean velocity (> 2 m/s)	Yes
Removed adjacent ensembles with unrealistically large change in velocity	Yes
Truncated bins based on largest/smallest	0.25% outliers

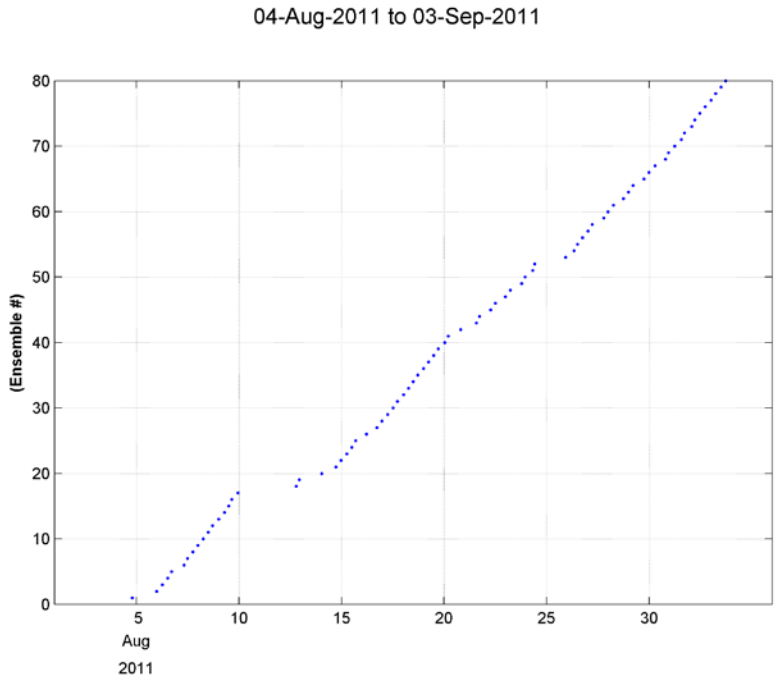

Figure 4. Temporal distribution of final averaged vessel-mounted ADCP data ensembles for the 4 August through 3 September period. Data gaps are associated with poor data quality associated with heavy seas.

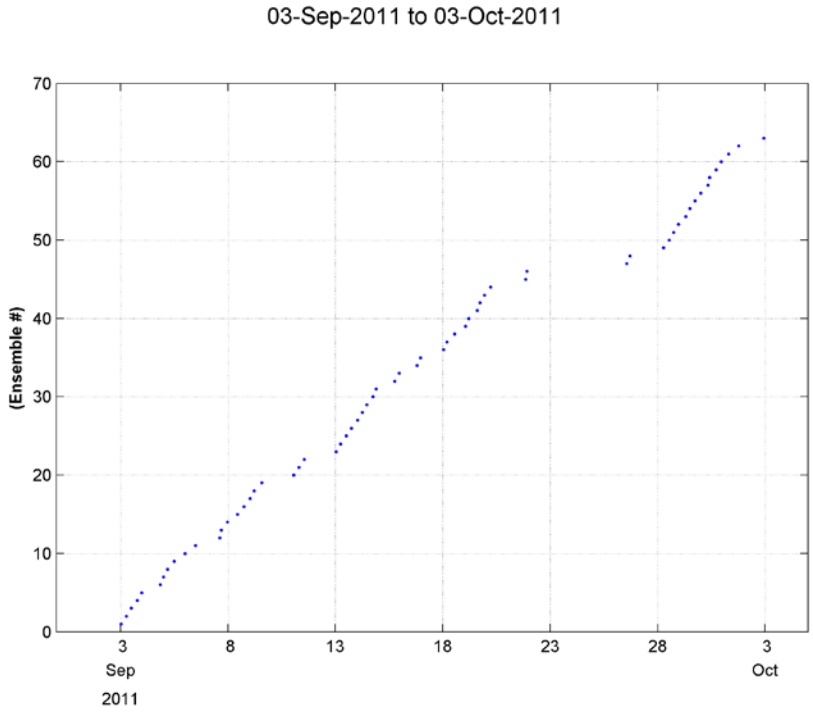

Figure 5. Temporal distribution of final averaged vessel-mounted ADCP data ensembles for the 3 September to 3 October period. Data gaps are associated with poor data quality associated with heavy seas.

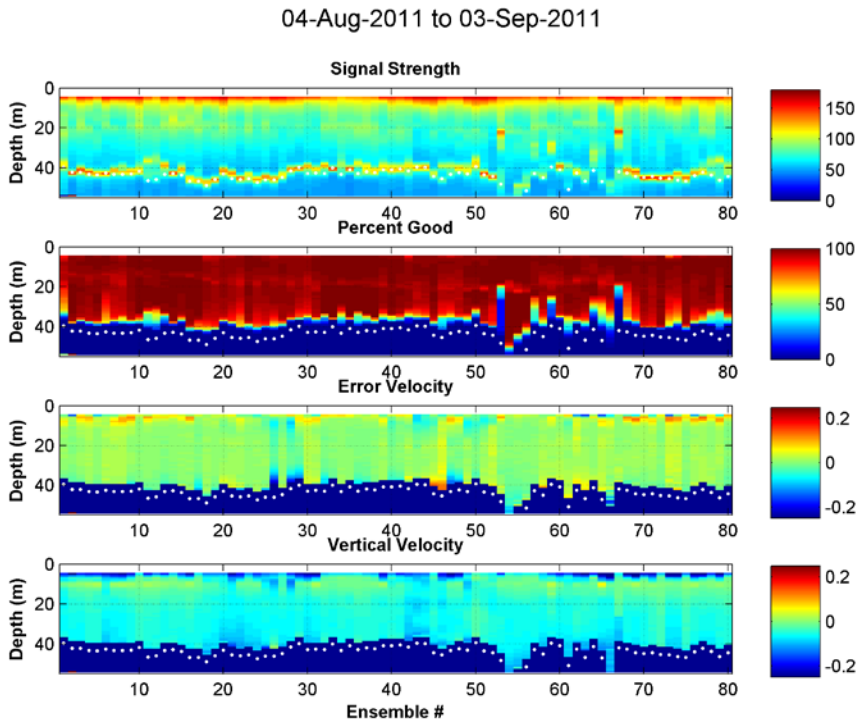

Figure 6. From top-to-bottom, signal strength, percent good, error velocity and vertical velocity of the 6-hourly averaged ensembles for 4 August – 3 September, 2011.

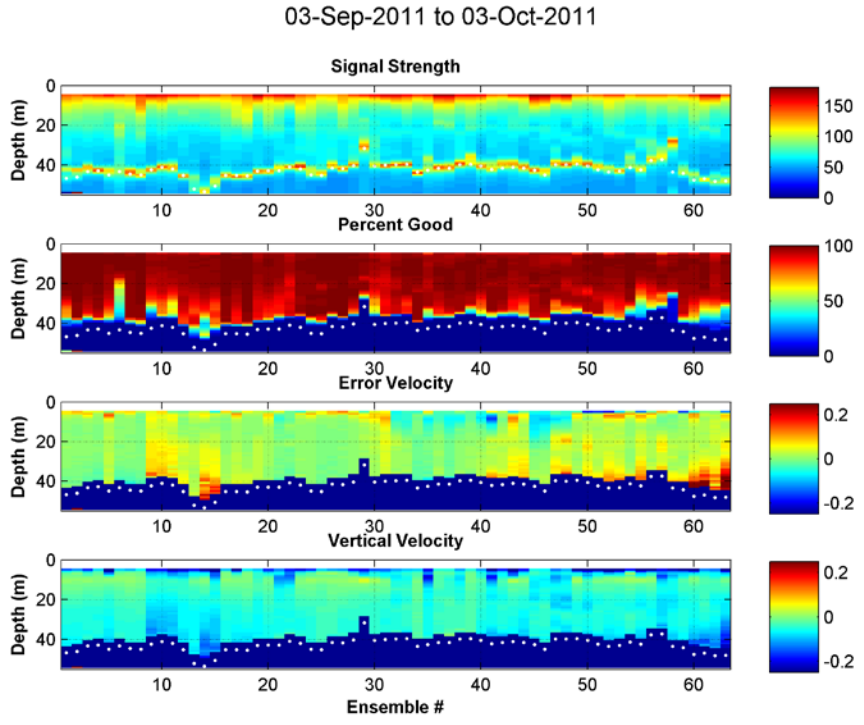

Figure 7. From top-to-bottom, signal strength, percent good, error velocity and vertical velocity of the 6-hourly averaged ensembles for 3 September to 3 October, 2011.

Results

Winds and Sea Ice 2008 - 2010

Figure 8 shows time series of the 3-hourly wind vectors from 1 June through 15 October from 2008 – 2011 from the NARR gridpoint within Burger (similar results hold for the Klondike and Statoil). The winds, while variable, were primarily from the northeast in all years. The patterns of variability among years are of interest, however, and may be of some importance in the seasonal evolution of the sea ice and water properties. In 2008 winds were from the northeast at 5 - 10 m s^{-1} (10 – 20 kts) from early July through early October except for a brief period of southwest winds in late July. In 2009, winds were from the northeast through July and then generally mild or from the southwest through early September. However, strong northeasterlies developed by the second week of September and these remained strong until mid-October. In 2010, strong northeasterlies prevailed in June, but in comparison to the other years, the winds from July through September were variable and weaker. In 2011, winds were primarily from the northeast from June through mid-October with only brief interludes of winds from the southern quadrant. Average wind speeds for the August - September period were the largest in 2011 being nearly double the speeds of 2009 and 2010.

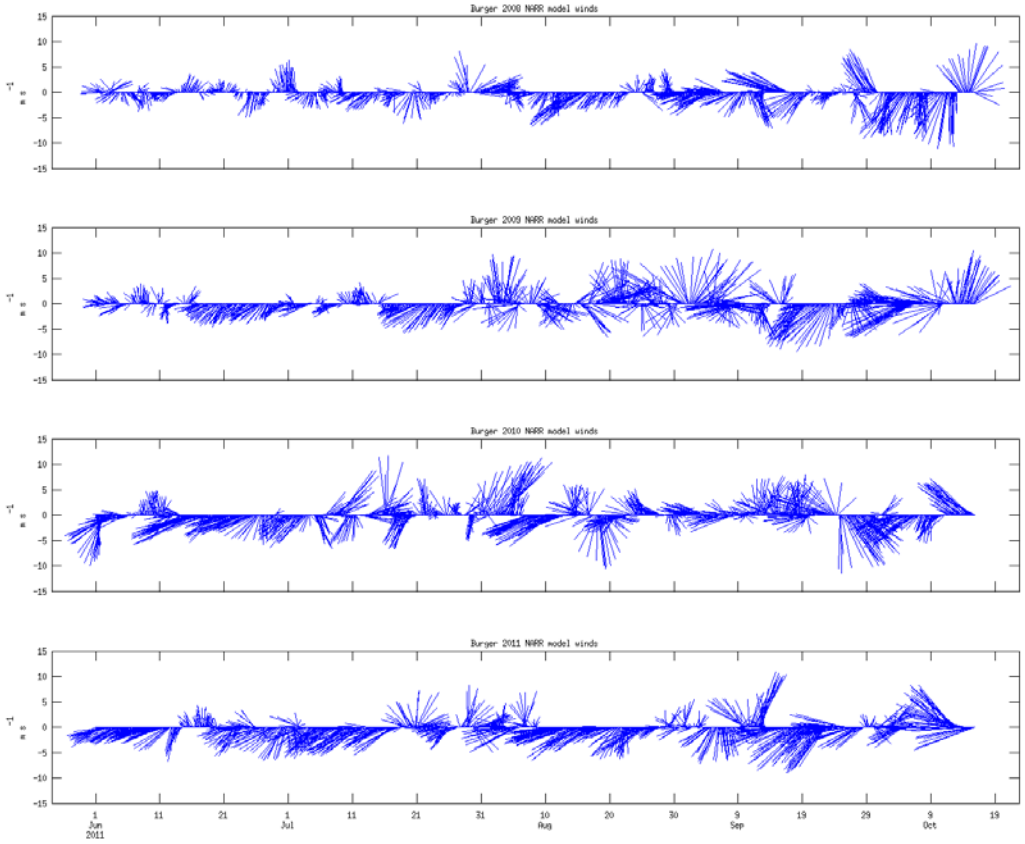

Figure 8. Vector “sticks” of 3-hourly for 2008 (top), through 2011 (bottom).

Sea ice concentrations

The seasonal distribution and retreat of sea ice also varied among the years. We illustrate this based on ice concentration data from the Advanced Microwave Scanning Radiometer - Earth Observing System (*AMSR-E*) satellite sensor and processed according to Spreen et al., (2008). We show ice concentration maps for 2011 for May, June, and July in **Figure 9** to provide a broader perspective of the seasonal evolution in sea ice retreat over the Chukchi shelf prior to the vessel surveys

In early May (**Figure 9**) a narrow band of open water developed offshore of the northwestern coast coincident with the beginning of sea ice retreat in Bering Strait. The opening along the northwest coast changed but little through the middle of May, although ice slowly retreated northward from the Strait. By 20 May (not shown) ice retreat accelerated westward offshore the northwestern coast of Alaska and northward from Bering Strait, such that by 25 May most of the region south of 69°N and east of 170°W was ice-free. However, ice concentrations of between 0 and 75%, remained along the coast north of the Seward Peninsula and west of the Lisburne Peninsula. By 10 June, most of the area south of 70°N and east of 170°W was ice free. For the northeast Chukchi Sea this represents a retreat of ~8cm day^{-1} for the region between 69°N and 70°N. The ice edge remained nearly stationary from mid-June through early July, with a prominent ice tongue, with concentrations of ~50%, extending southwestward from Hanna Shoal. The tongue largely disappeared and the ice edge, although very compact, had retreated to ~72°N by 5 July (not shown). Ice retreat continued more slowly thereafter, with the principal change being a large decrease in ice concentrations around 72°N from 100% (July 5) to 50 – 75% ice cover by 10 July. Ice decay and retreat accelerated rapidly thereafter so that by the end of July the region was effectively ice-free.

Although the pattern of ice retreat in 2011 was similar to that observed in 2010, the rate of ice retreat in 2011 was much faster than in 2010. This is evident upon comparing **Figure 9** with **Figure 10**, which shows July ice concentration maps for similar dates in the other years. Note that in the previous years more ice remained over the shelf by late July, particularly in the vicinity of Herald and Hanna Shoal, in comparison to 2011. The absence of ice over these regions in July 2011 would suggest that meltwater concentrations were substantially reduced in 2011 compared to other years. Indeed, this is borne out by the CTD data discussed later.

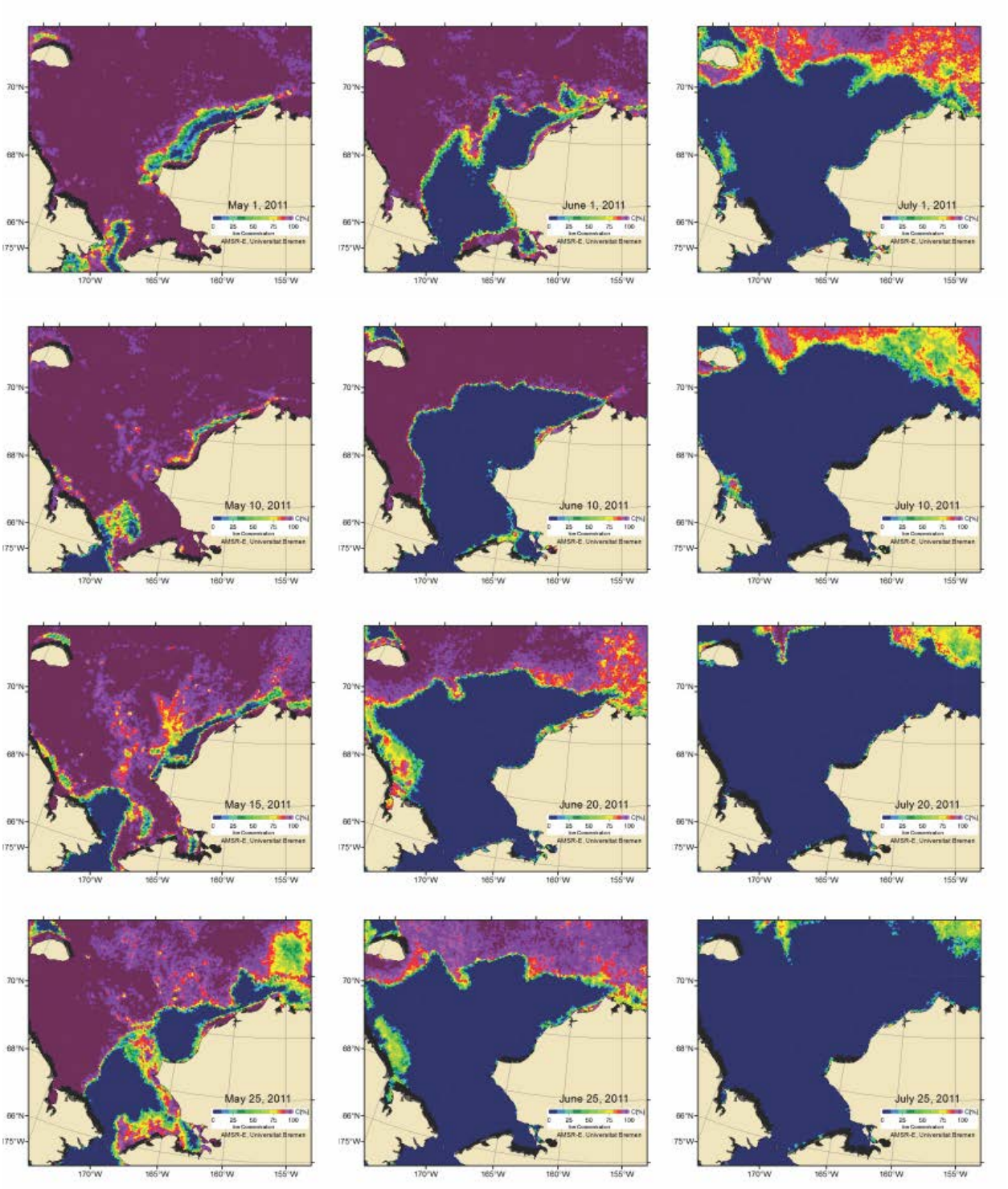

Figure 9. AMSRE-E sea ice concentration maps for the Chukchi shelf in 2011: May (left column), June (middle column) and July (right column).

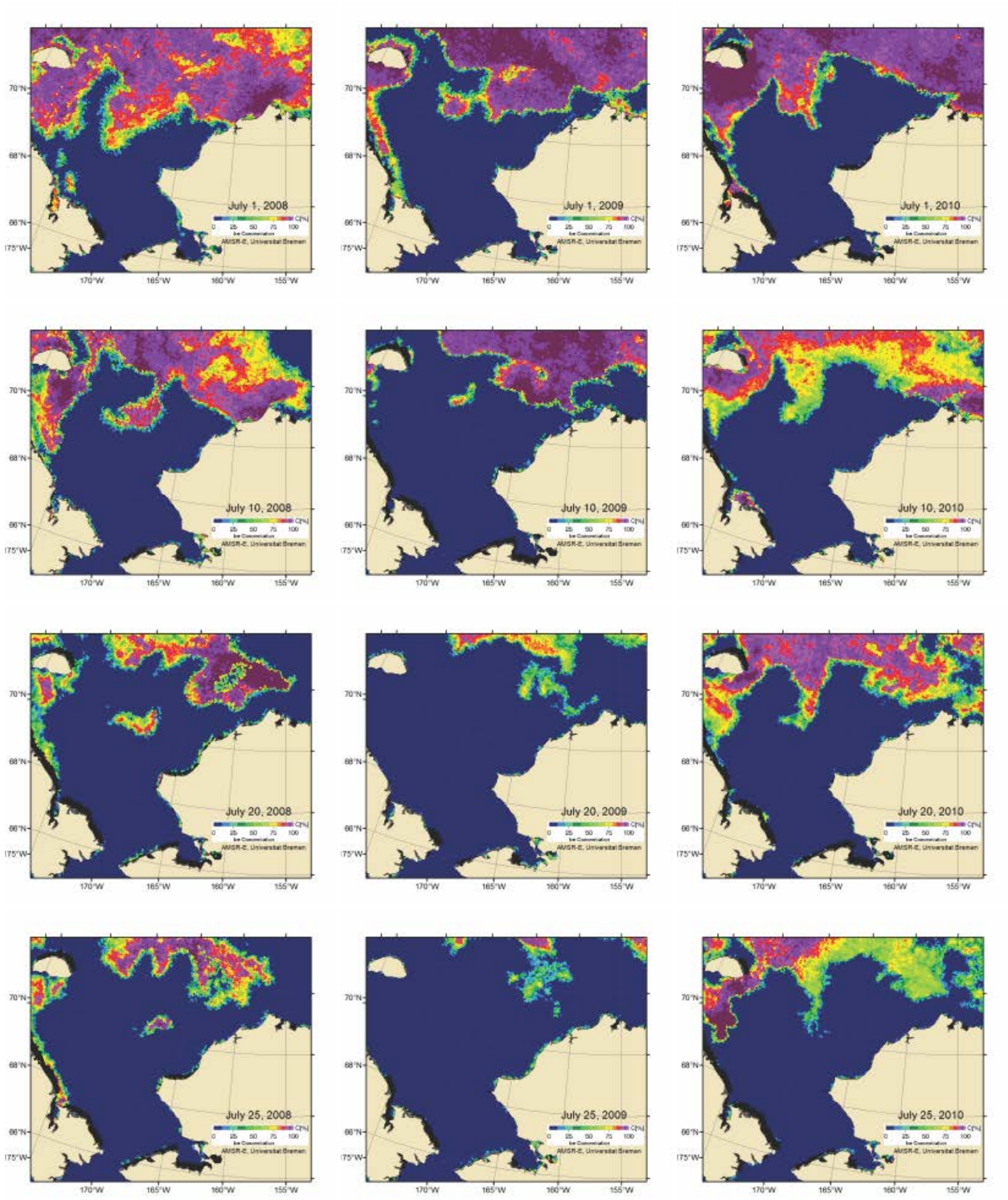

Figure 10. AMSRE-E sea ice concentration maps for the Chukchi shelf throughout July 2008 (left column), 2009 (middle column) and 2010 (right column).

Results: 2011 Survey

Temperature and salinity

Before presenting the spatial distribution of temperature and salinity along the CTD transects we first describe the various water masses observed in the survey areas (**Figure 11**). The figure is a T/S diagram (scatterplot) depicting the temperature (T) and salinity (S) characteristics at each 1-meter averaged CTD sample from all casts. The data are segregated into stations located in the study areas during the first and second cruises (left and middle panels, respectively) and those outside of the study areas during the third cruise (right panel). The rightmost panel is arbitrarily segregated into stations south and north of Hanna Shoal and those located between these two groupings. The results are remarkably different from previous years in two key respects. First, there appears to be very little geographic or temporal variation in the T/S properties. Later we will show that this is not completely true. Nevertheless, the T/S variability in 2011, was much less than in previous years. For example, the coldest [<0°C] and saltiest [>32] waters are found in Burger and Statoil.) Second, unlike previous years there is no cool, dilute water (generally with temperatures <3°C and salinities <30). Waters with these properties reflect the influence of ice meltwater in T/S space. The absence of distinct meltwater signatures in 2011 is consistent with the rapid retreat of ice mentioned above. Hence by the time of the first survey, any remaining meltwater in the area had either been advected away and/or had mixed with saltier water and warmed. By contrast in previous meltwater was always a prominent feature in early August (and often in late August and early September) and that there was considerable geographic variability in water properties among the various survey sites.

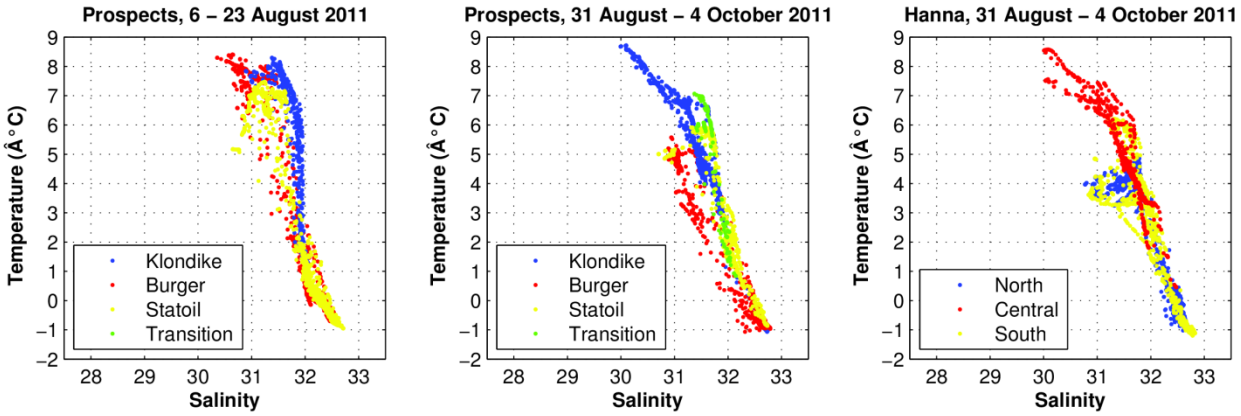

Figure 11. Temperature-salinity diagrams for each survey conducted in 2011. The left and middle panels are the T/S plots for the survey areas only. The rightmost panels are data collected during the second cruise from stations outside of the survey areas.

We next investigate the temperature, salinity, density, and fluorescence distributions as a function of distance and depth (pressure) along a number of transects across the region. **Figures 12 and 13** show the locations of transects used in these constructions for both cruises. The transects selected can be easily compared with those in previous reports and/or provide a comprehensive depiction of the spatial distribution of water properties over the region.

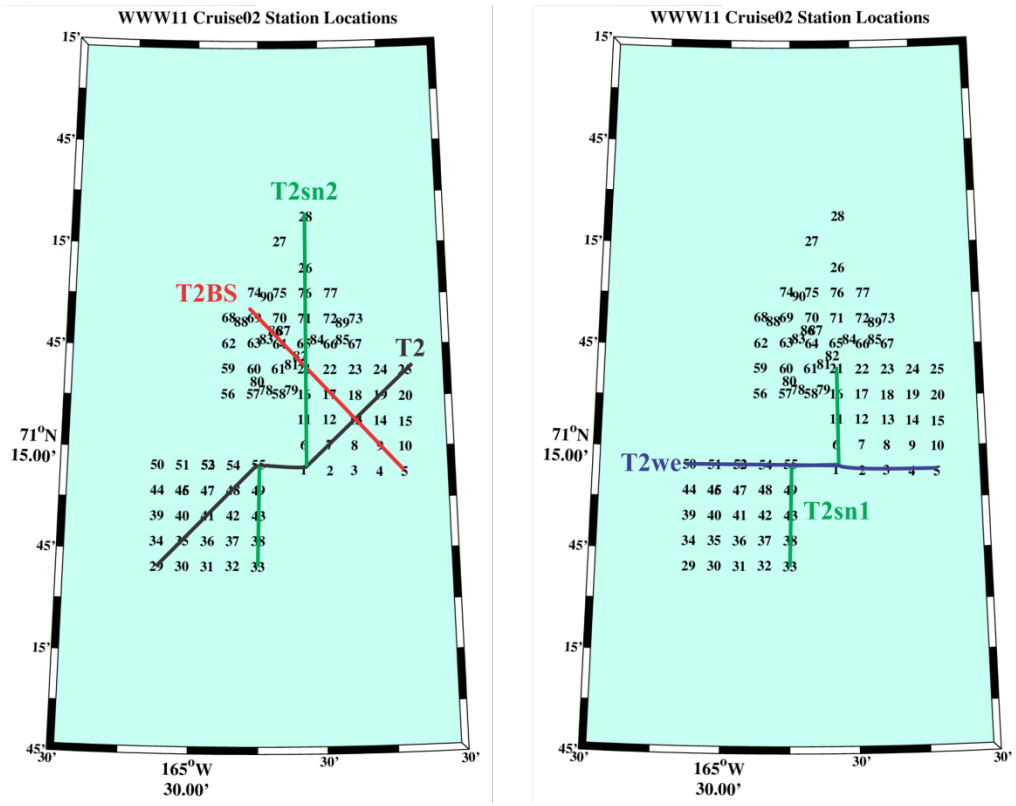

Figure 12. The distribution of stations during the 6 – 23 August 2011 survey. The various labeled lines were used to construct the transects discussed below.

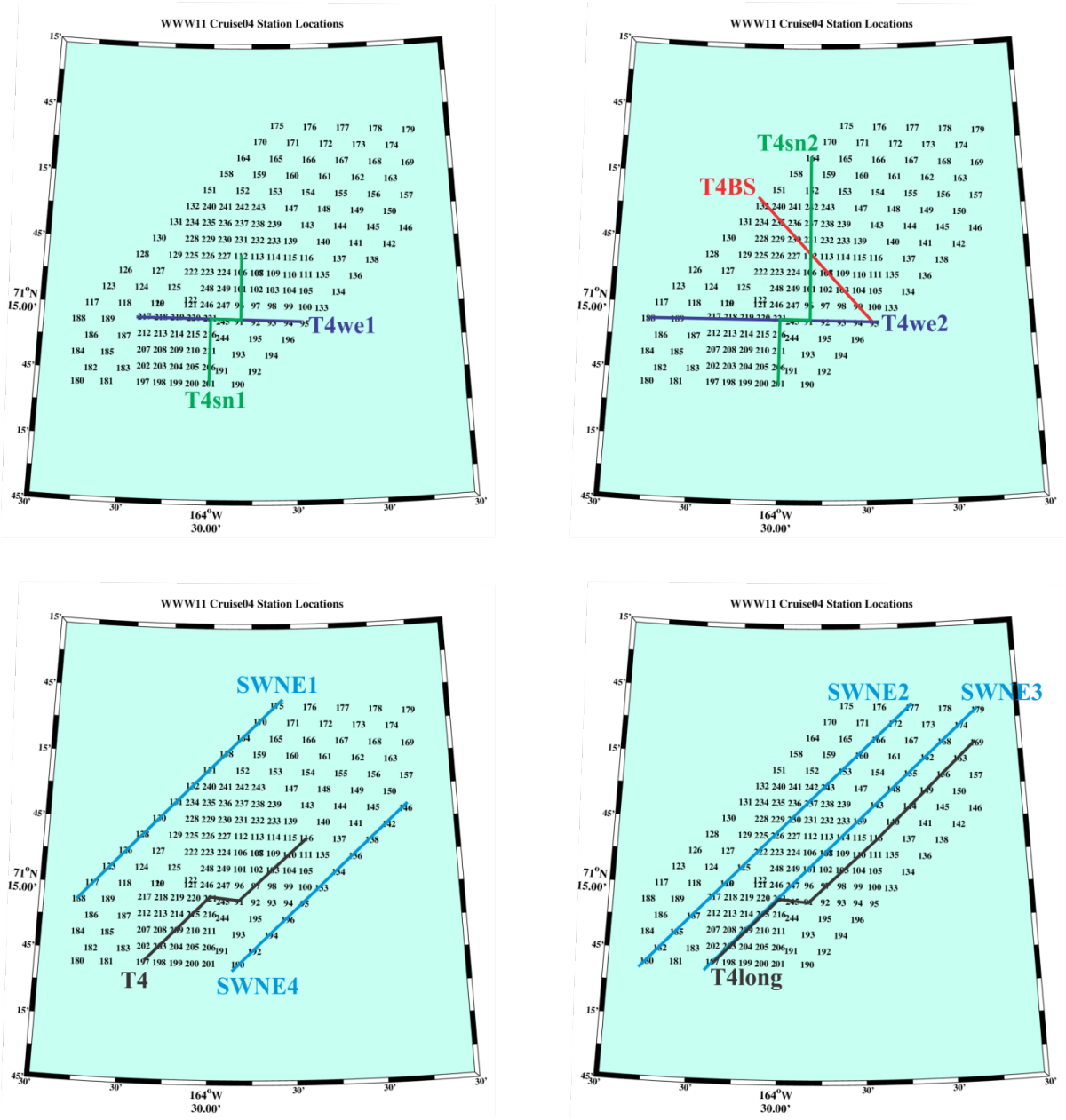

Figure 13. The distribution of stations during the 31 August – 4 October 2011 survey. The various labeled lines were used to construct the transects discussed below.

Water Property Distributions

The spatial distributions of water mass properties for the 6 – 23 August 2011 (WWW11 Cruise 02) and for the 31 August – 4 October (WWW11 Cruise 02) survey are shown in **Figures 14 – 22** along sections T2we (west-east), T4we1, T4we2, T2sn1 (south-north), T2sn2, T4sn1, T4sn2, T2 and T4 (southwest-northeast across Klondike and Burger) and T2BS and T4BS (southeast to northwest from Burger to Statoil), respectively. Each transect is represented by four panels that

show temperature (°C), salinity (unitless), sigma-t (a scaled variable for water density), and fluorescence (volts); the latter being a relative measure of chlorophyll biomass.

The temperature structure across the T2we section (**Figure 14**) consisted of warm (>7°C) surface waters uniformly distributed across the entire section and down to a depth of about 10 – 15 m. Below the surface layer, temperatures decreased rapidly across the thermocline and were ~2°C at ~ 25 m. At greater depths, temperatures were vertically homogeneous and ≤1.5°C, with the coldest waters (≤0.5°C) found midway along the southern boundary of Burger. Surface salinities ranged from 30.5 to <31.5, with the freshest water at the easternmost end of the transect. Subsurface (>20 m depth) salinities ranged between 31.5 and 32.5, and showed little horizontal variation. The 10 m thick pycnocline, centered between 15 and 20 m, was largely due to the vertical temperature gradient. Fluorescence was negligible (<0.25 v) above the pycnocline and over most of the section, except within the pool of high salinity (>32) water along the western end of the section.

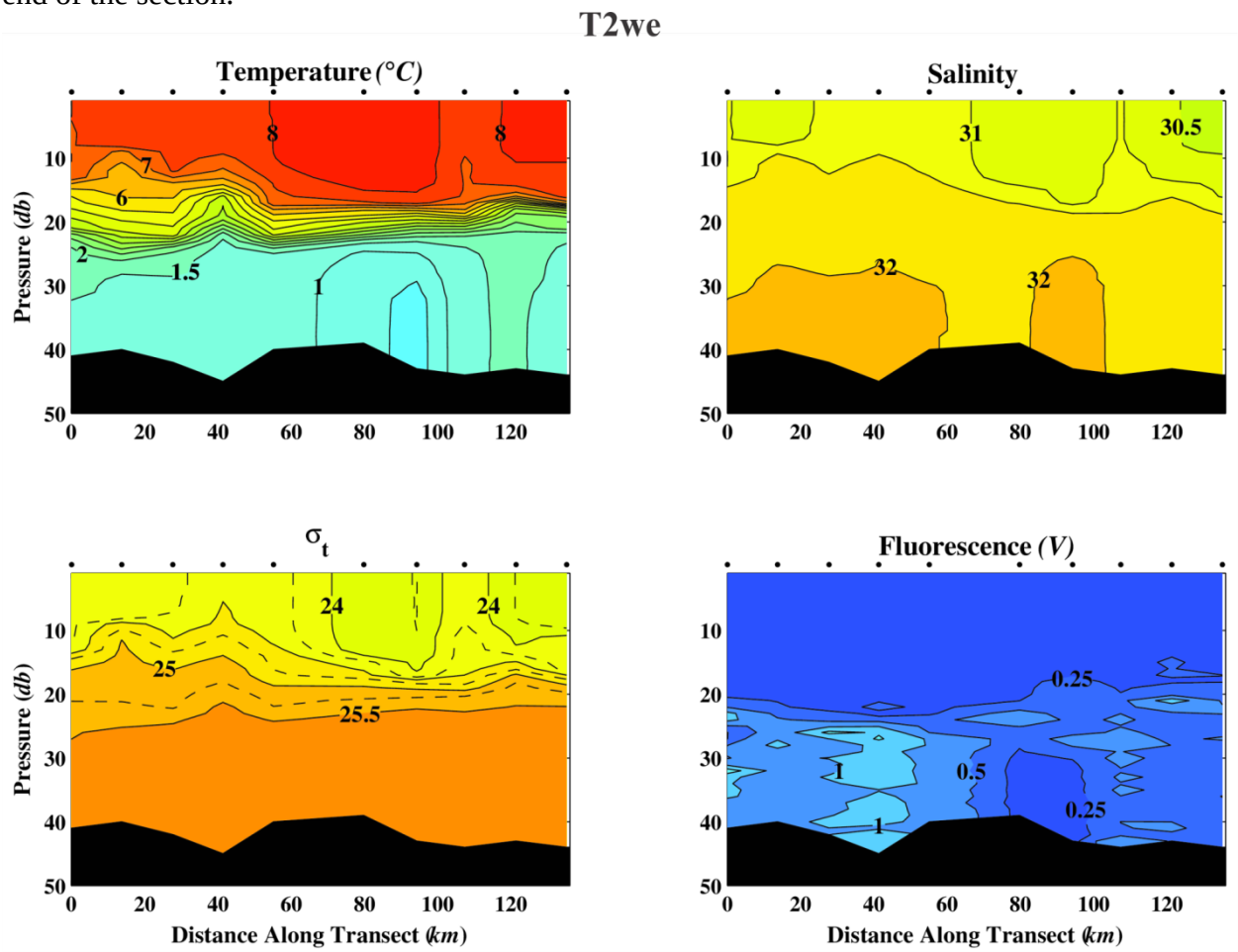

Figure 14. West-east (T2we) section (per figure 12) of temperature (upper left), salinity (upper right), sigma-t (lower left), and fluorescence (lower right) from the 6 – 23 August 2011 survey.

Substantial changes occurred along this transect by late August and early September (**Figure 15**). Surface waters had cooled, although not uniformly. Along the western end of Klondike temperatures decreased from 8 to 7°C, while along the eastern end of the transect temperatures decreased from 8 to ~4°C. Upper ocean salinity changes were negligible, however. Subsurface

temperatures and salinities had also changed. Over the western end of the transect temperatures increased from 1.5°C to ~3°C and salinities decreased from >32 to <32. Within Burger, over the eastern end of the transect, temperatures decreased from ~1°C to ~-0.5°C and salinities increased to >32.5.

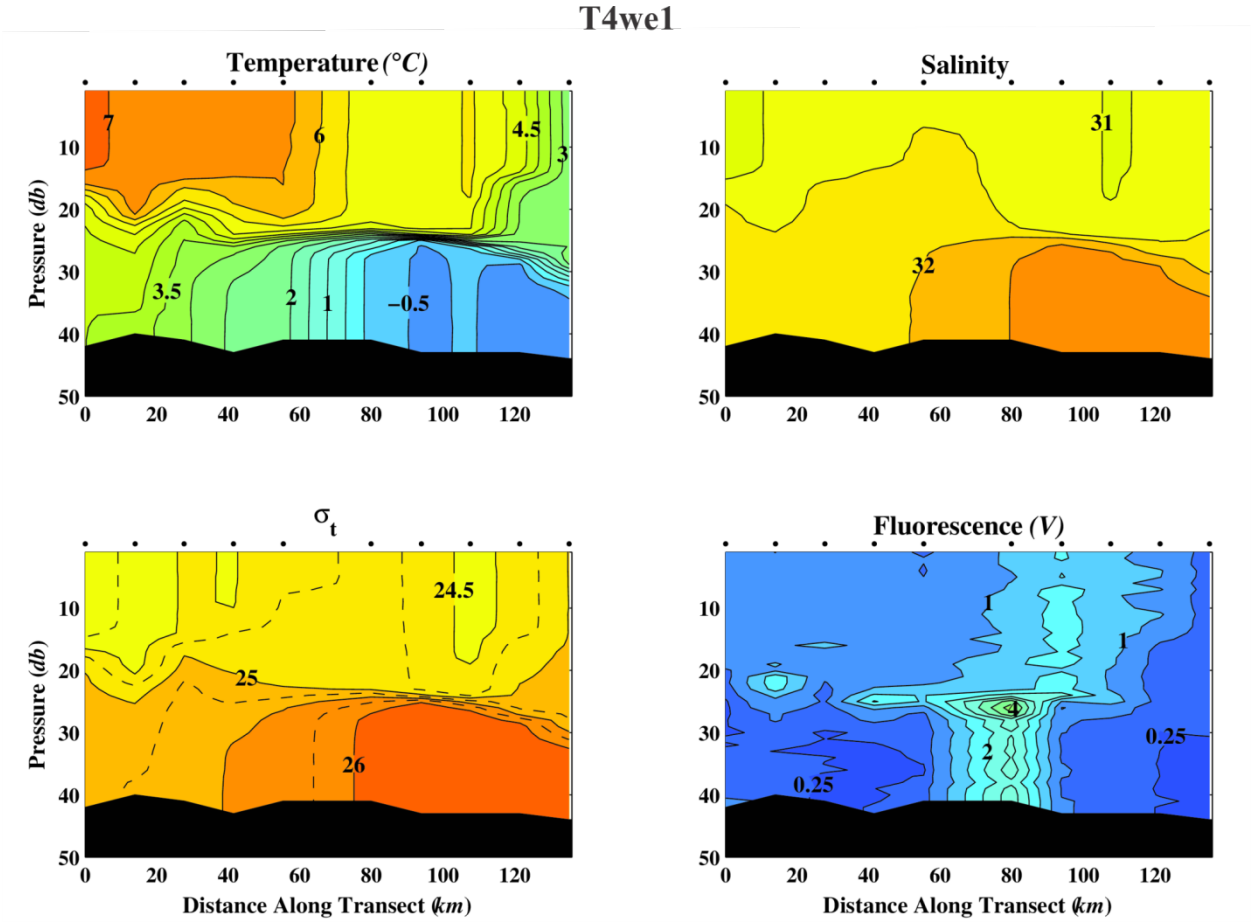

Figure 15. West-east (T4we1) section (per **Figure 13**) of temperature (upper left), salinity (upper right), sigma-t (lower left), and fluorescence (lower right) from the 31 August – 4 October 2011 survey. The stations used in this section have locations identical to those used in constructing **Figure 14**.

Figure 16 shows the same transect in late August and early September, but includes two additional stations to the west of the transects shown in **Figures 14** and **15**. These stations, which lie within the Central Channel, had surface properties similar to those within Klondike, however, the subsurface waters were both cooler and saltier than those along the west side of Klondike.

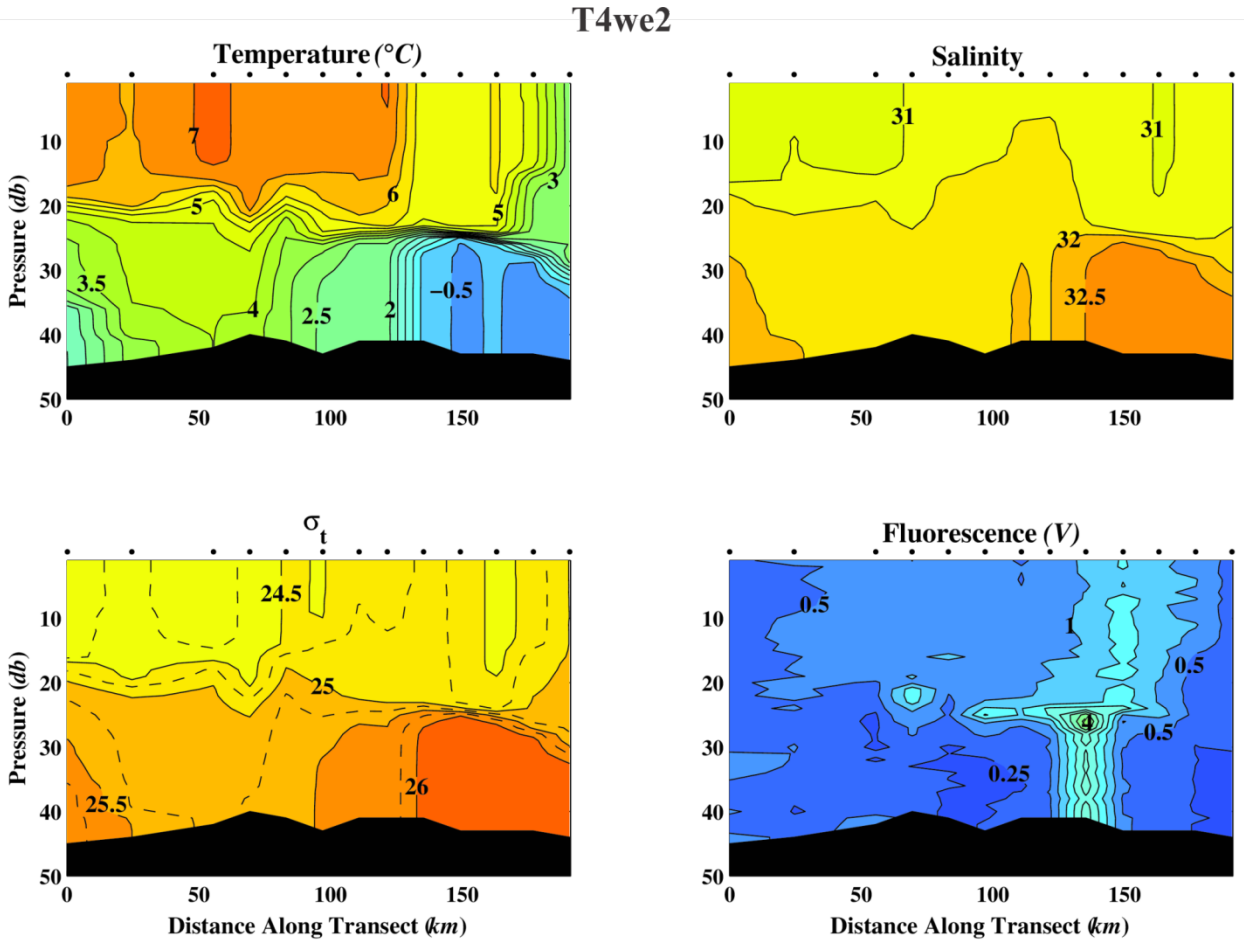

Figure 16. West-east (T4we2) section (per figure 13) of temperature (upper left), salinity (upper right), sigma-t (lower left), and fluorescence (lower right) from the 31 August – 4 October 2011 survey.

Sections T2sn1 and T2sn2 (**Figures 15 and 16**) and sections T4sn1 and T4sn2 (**Figures 17 and 18**) are composed of identical stations except the "sn2" sections extend farther north, and include a portion of the south side of Hanna Shoal. In the first survey, temperatures decreased by ~8°C to 6°C from south to north in the upper ~20 m. Subsurface temperatures were ~2°C in Klondike, but decreased to -0.5°C in Burger and on the north side of the Shoal. The subsurface thermal front at ~km 60 along coincided with a northward increase in salinity from <32 to >32, with deep salinities exceeding 32.5 at the northern end of the T2sn2. This cold, high salinity tongue is the "winter water" formed the previous winter during freezing and ice-formation. Surface salinities varied little over the section and ranged from 30.5 to 31.5. The pycnocline was rather weak over the southern (Kondike) end of the transect, but strengthened within Burger and to the north. Within Klondike, the pycnocline was primarily a function of the vertical temperature gradient since salt stratification was extremely weak. Fluorescence was patchy, with the highest values below the pycnocline and along the northern end of the transect. The highest fluorescence values were found slightly below the pycnocline in Burger on both surveys.

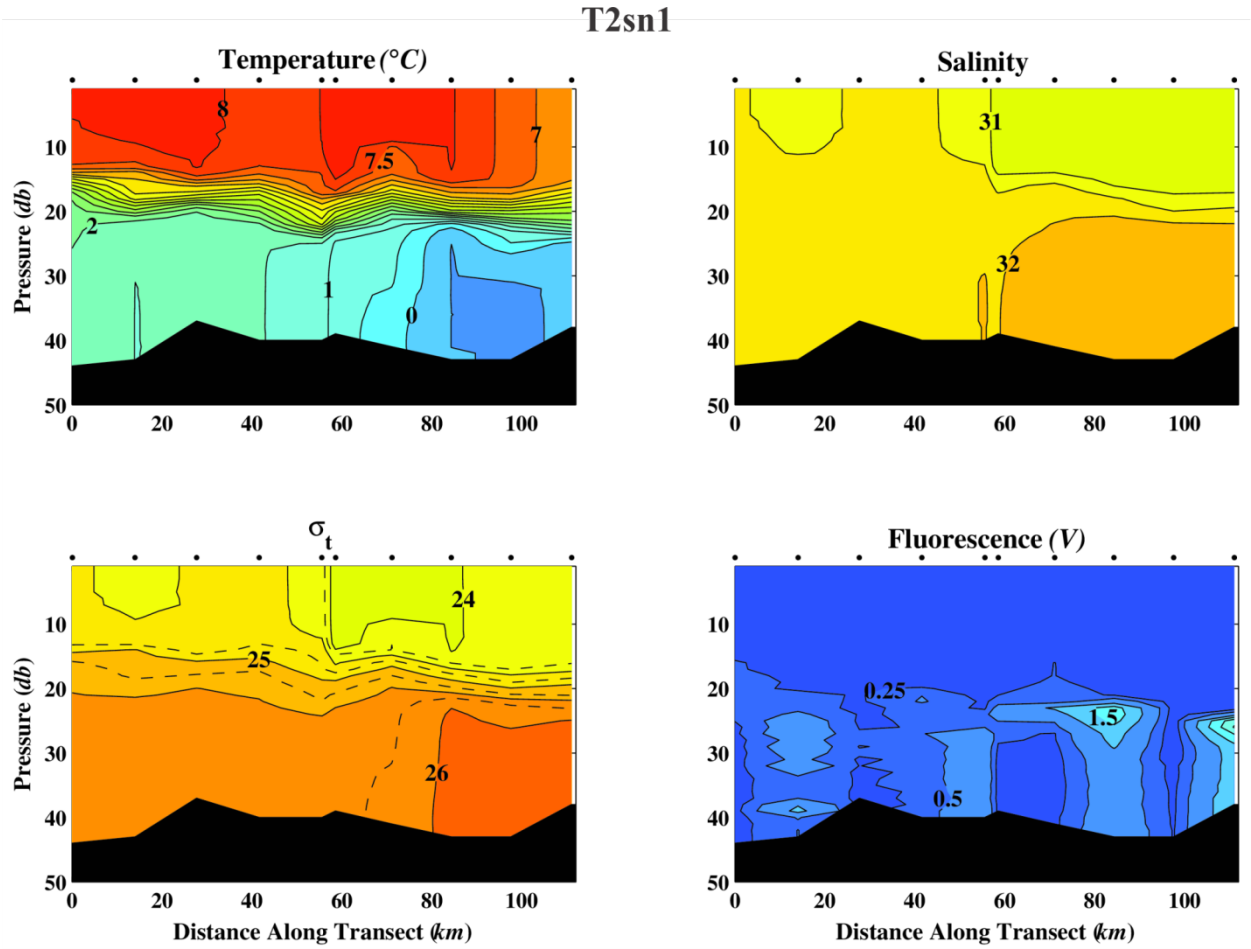

Figure 15. South-north (T2sn1) section (per figure 12) of temperature (upper left), salinity (upper right), sigma-t (lower left), and fluorescence (lower right) from the 6 – 23 August 2011 survey.

During the second survey (**Figures 17 and 18**) surface temperatures had cooled by ~1 to 2°C. However, subsurface temperatures had increased from 2°C to 3.5°C in Klondike. Here, the stratification remained primarily temperature-dependent, but weakened due to cooling at the surface and warming at depth. There was, however, very little change in the surface and subsurface properties (including the stratification) within the Burger portion of this transect. On the other hand, there were substantial changes in subsurface water properties north of Burger as seen upon comparing **Figures 16 and 18**. During the first survey this region was uniformly occupied by winter water with temperatures of ~-0.5°C and salinities >32.5. Nearly all of this water was replaced by warmer and fresher waters by the time the second survey occurred. Indeed the only pocket of winter water along this transect occurred within Burger.

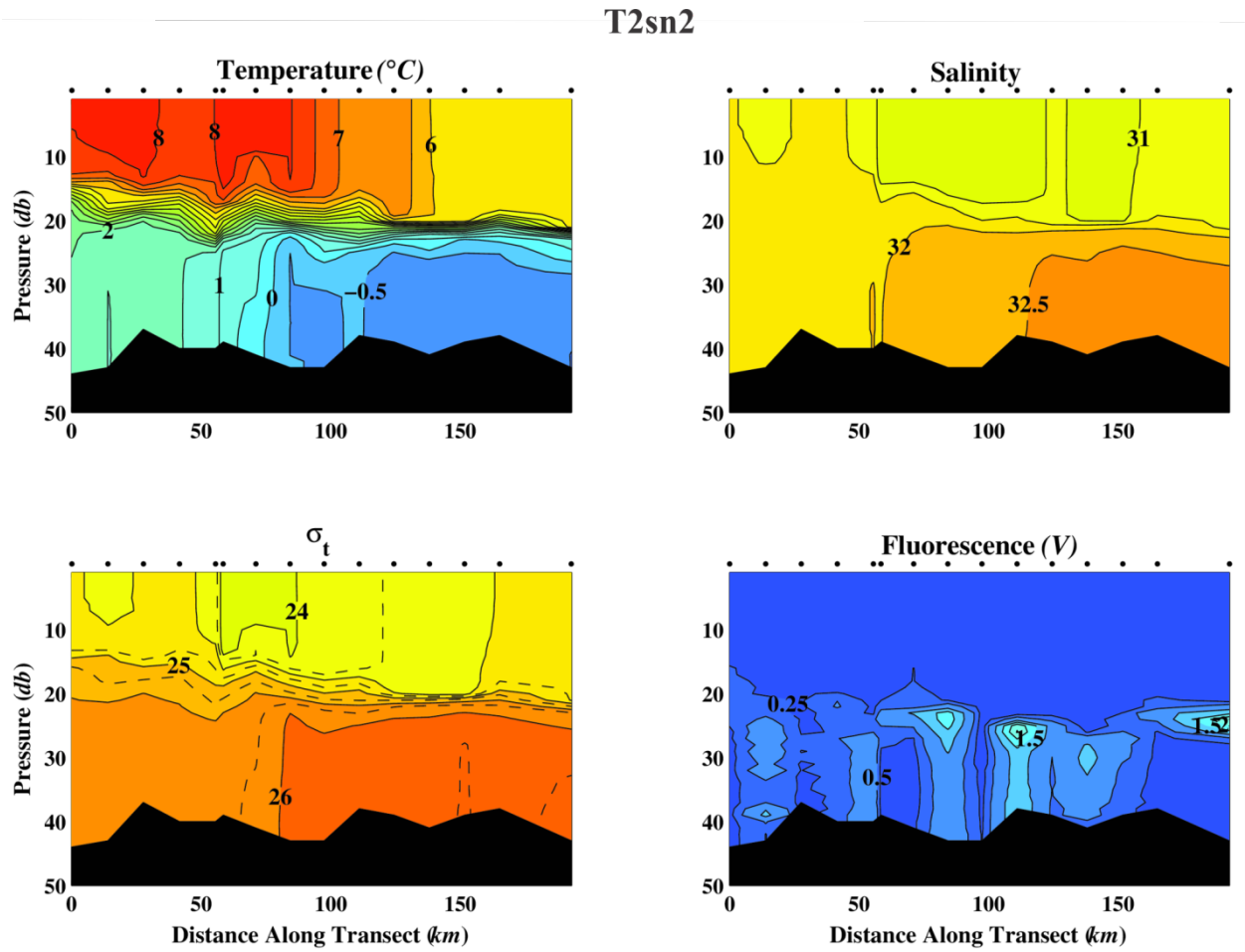

Figure 16. South-north (T2sn2) section (per figure 12) of temperature (upper left), salinity (upper right), sigma-t (lower left), and fluorescence (lower right) from the 6 – 23 August 2011 survey.

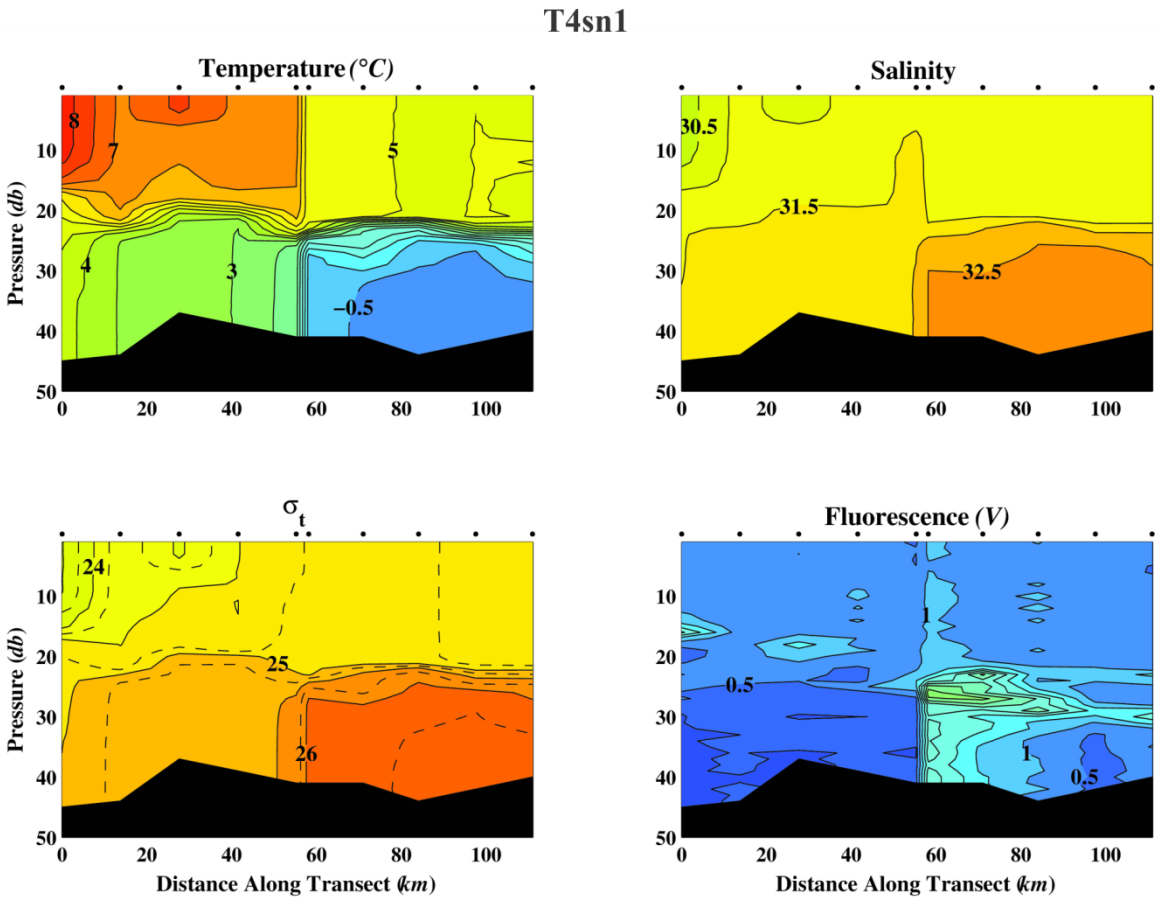

Figure 17. South-north (T4sn1) section (per **Figure 13**) of temperature (upper left), salinity (upper right), sigma-t (lower left), and fluorescence (lower right) from the 31 August – 4 October 2011 survey.

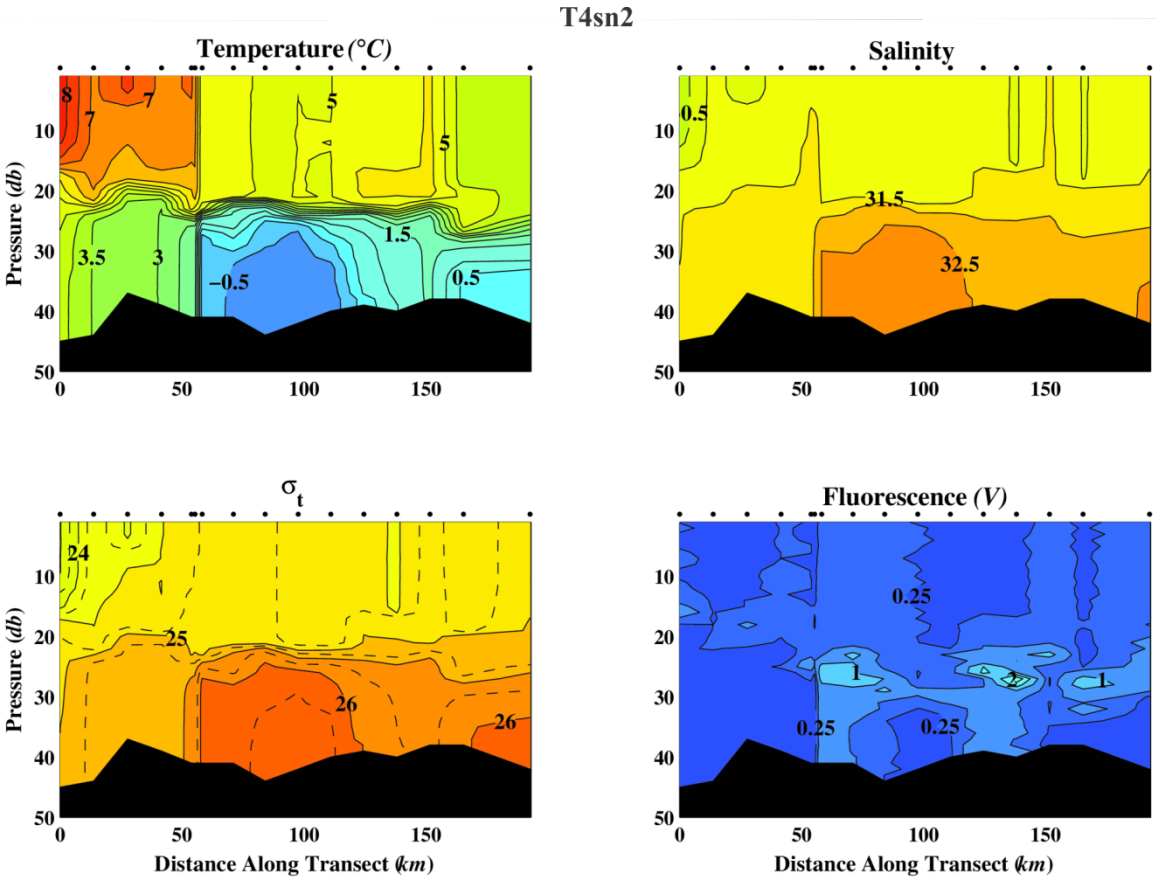

Figure 18. South-north (T4sn2) section (per **Figure 13**) of temperature (upper left), salinity (upper right), sigma-t (lower left), and fluorescence (lower right) from the 31 August – 4 October 2011 survey.

Sections T2 (**Figure 19**) and T2BS (**Figure 21**) are nearly orthogonal to one another and cross within Burger (**Figure 12**). The water properties are similar to those described above with respect to the near-uniformity in upper layer and pycnocline properties. Within the lower layer we find that the coldest and saltiest waters are in the middle and northern half of Burger (right hand sides of both **Figures 19 and 21**), while warmer and less salty waters occur along the bottom in Klondike and Statoil. The corresponding transects from the 31 August – 4 October survey are shown in **Figures 20 and 22**. Surface layer changes were similar to those described above along both transects. There were however, remarkable changes in the bottom water properties within Burger and Statoil. The changes in Statoil, illustrated by comparing **Figure 20** with **Figure 22**, involved both warming and freshening between the two surveys. In contrast, comparisons between the two surveys indicate that the volume of cold, salty winter water increased in Burger between the two surveys, with these changes largely confined to the eastern half of this survey area. Fluorescence values on these transects had variable magnitudes with the largest values found during the second survey in the southwest corner of Burger (**Figure 20**) and the western half of Statoil.

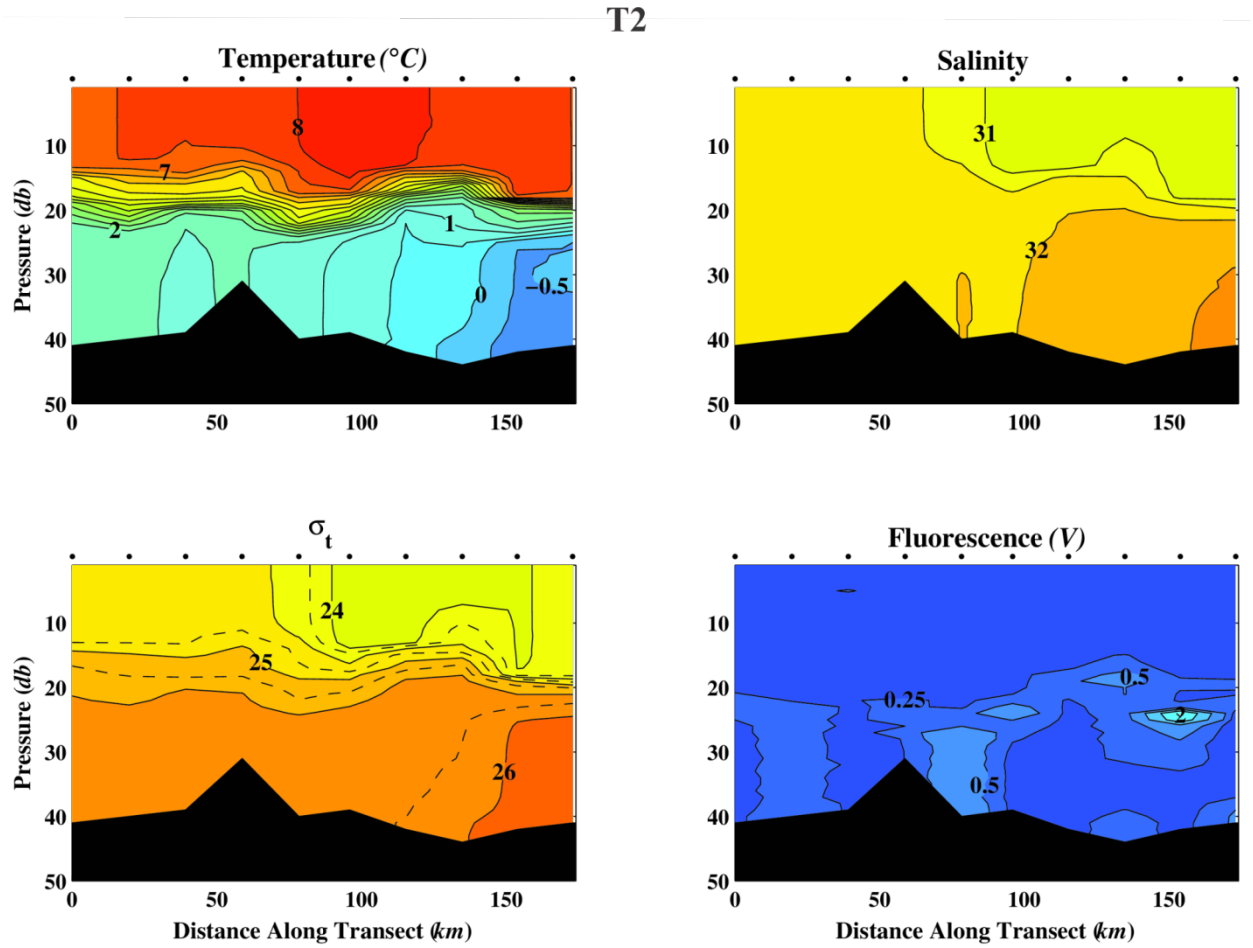

Figure 19. Southwest-northeast (T2) section (per figure 12) of temperature (upper left), salinity (upper right), sigma-t (lower left), and fluorescence (lower right) from the 6 – 23 August 2011 survey.

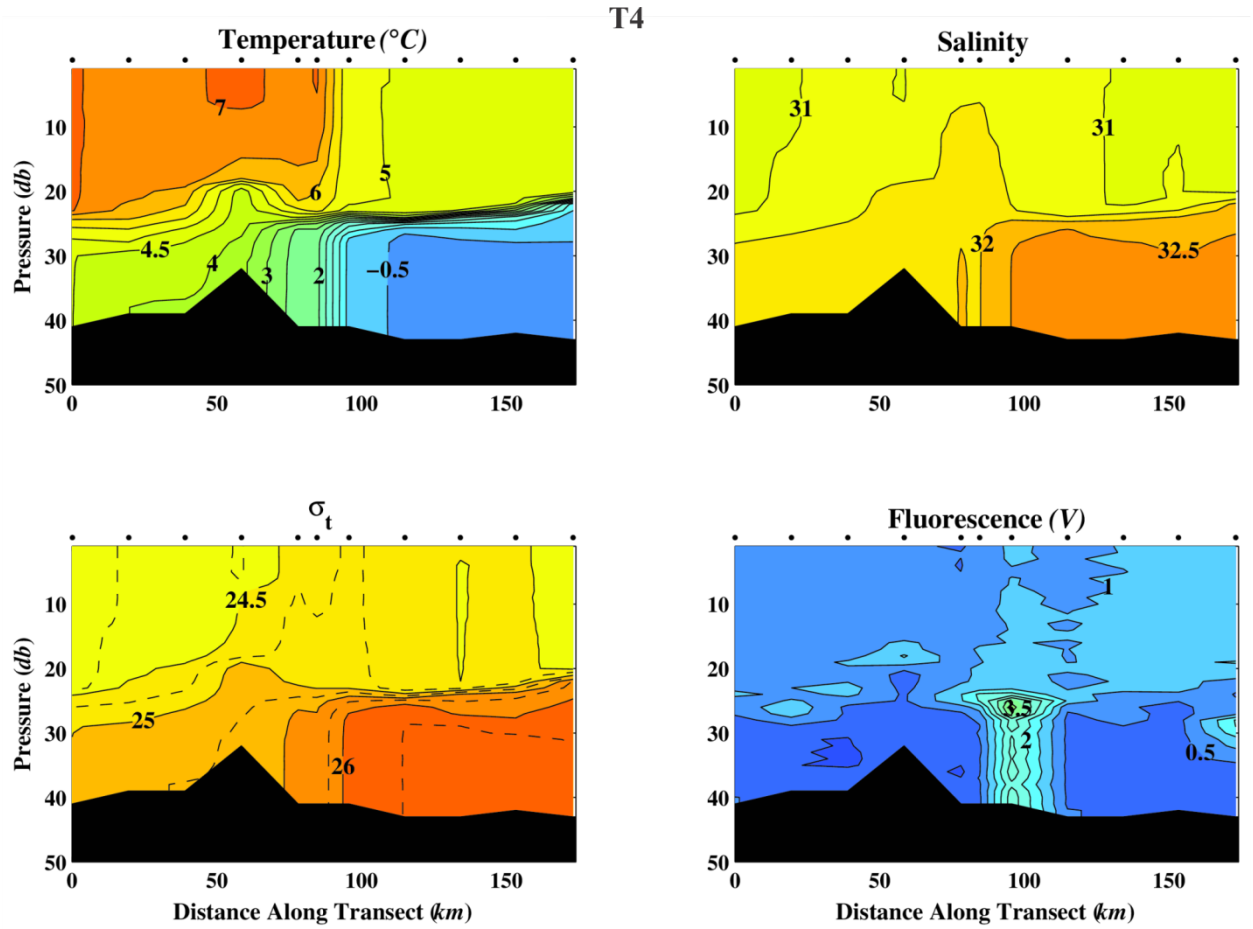

Figure 20. Southwest-northeast (T4) section (per **Figure 13**) of temperature (upper left), salinity (upper right), sigma-t (lower left), and fluorescence (lower right) from the 31 August – 4 October 2011 survey.

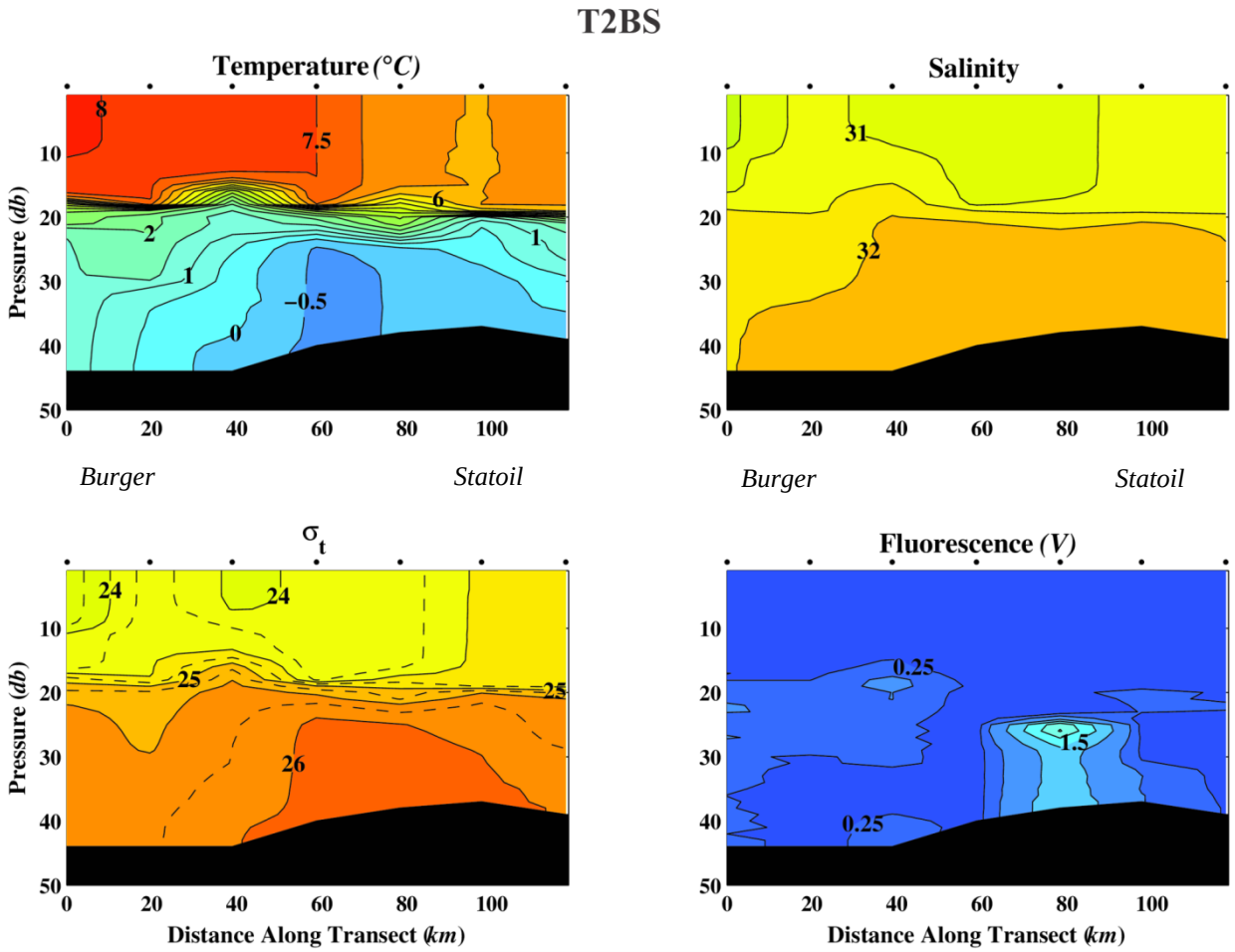

Figure 21. Southeast-northwest (T2BS) section (per figure 12) of temperature (upper left), salinity (upper right), sigma-t (lower left), and fluorescence (lower right) from the 6 – 23 August 2011 survey. Statoil (Burger) stations are left (right) of the center of the each figure.

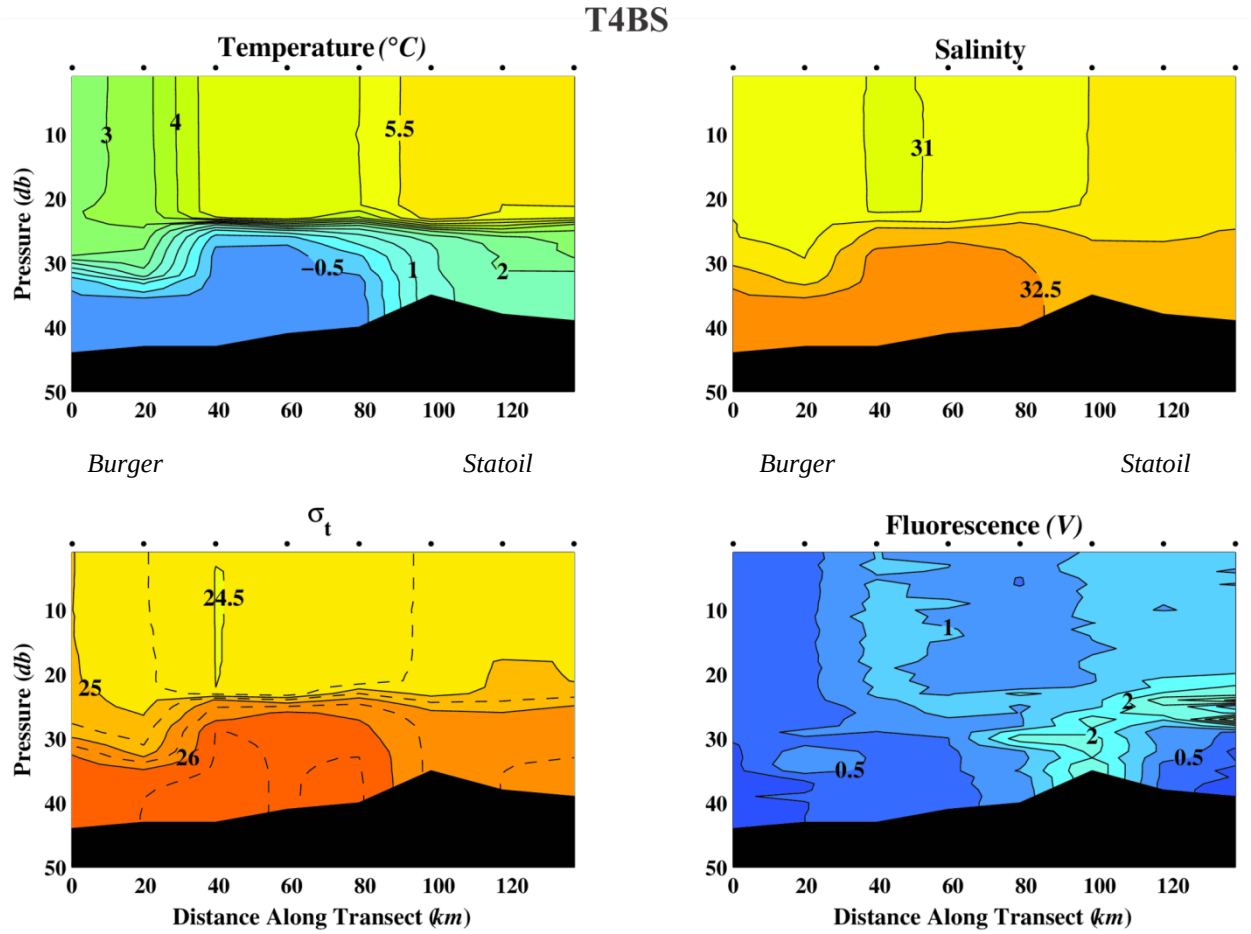

Figure 22. Southeast-northwest (T4BS) section (per **Figure 13**) of temperature (upper left), salinity (upper right), sigma-t (lower left), and fluorescence (lower right) from the 31 August – 4 October 2011 survey. Statoil (Burger) stations are left (right) of the center of the each figure.

The final sections discussed include SWNE1 (**Figure 23**), SWNE2 (**Figure 24**), SWNE3 (**Figure 25**), T4long (**Figure 26**), and SWNE4 (**Figure 27**). Each section extends from the southwest to the northeast and the presentation proceeds from the west (SWNE1) to east (SWNE4) across the broad survey region occupied only during the second cruise (see **Figure 13** for section locations). The transects cannot be regarded as synoptic because as noted previously (cf. Figure 3) the northern stations were occupied 2 -3 weeks after the southern stations. SWNE4 suffers the greatest aliasing insofar as the northeasternmost stations along this line were occupied ~4 weeks after the southeasternmost stations on this transect. Despite this caveat we make the following general statements:

1. There was little horizontal variation in upper ocean salinities, but surface temperatures were as much as 4°C warmer along the southern end of the transects compared to the northern end. The lowest salinities (<30.5) and warmest temperatures (7-8°C) were encountered at the southwest end of transect SWNE4 (**Figure 27**). Water with these properties are likely infiltrating into this area from the Alaskan Coastal Current.
2. Near-bottom water temperatures also decreased from south to north and bottom horizontal temperature gradients were as ~4°C/50 km. Maximum surface temperature gradients were <2°C/50 km and not coincident with the subsurface temperature gradients.

3. Winter water (temperature <0°C and salinity >32) was encountered on the northern end of each section, but the coldest (<-1°C) water observed was within or to the east of Burger on sections SWNE3 (**Figure 25**), T4long (**Figure 26)**, and SWNE4 (**Figure 27**). The vertical stratification tended to be greatest in the areas with coldest bottom waters.
4. Fluorescence levels were generally low, but patchy, with the highest values occurring below the pycnocline and associated with the cold, dense winter waters.

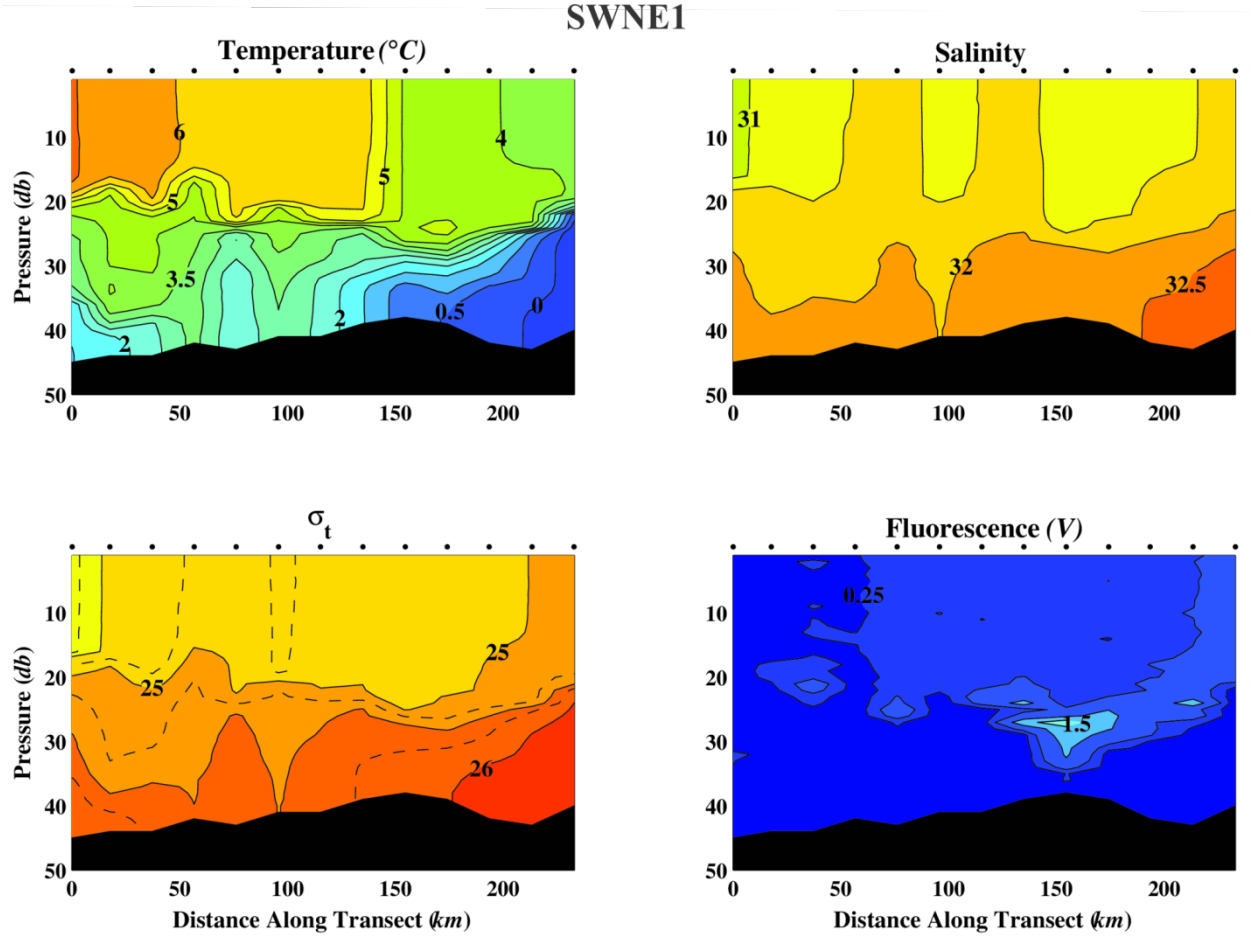

Figure 23. Southwest-northeast (SWNE1) section (per **Figure 13**) of temperature (upper left), salinity (upper right), sigma-t (lower left), and fluorescence (lower right) from the 31 August – 4 October 2011 survey.

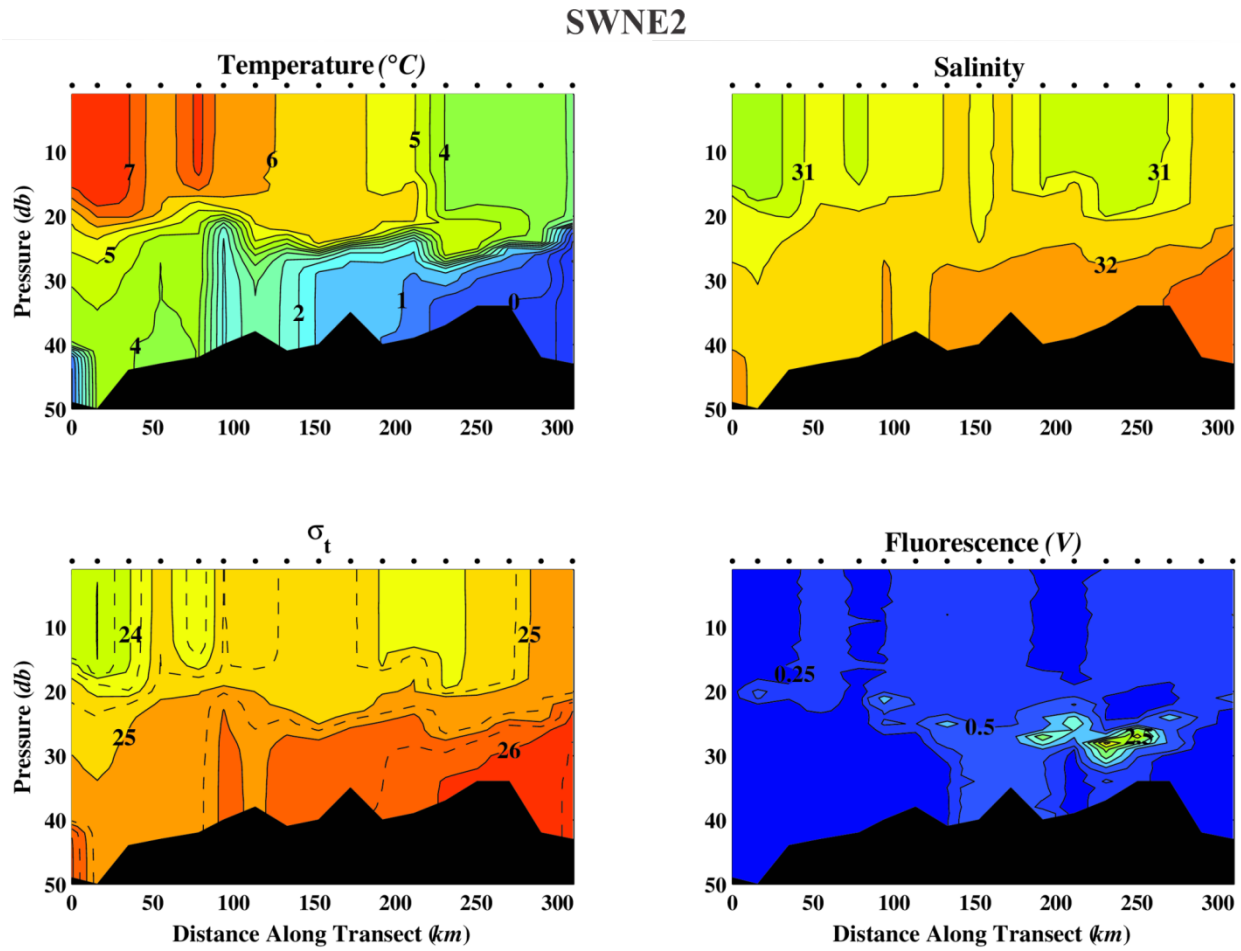

Figure 24. Southwest-northeast (SWNE2) section (per **Figure 13**) of temperature (upper left), salinity (upper right), sigma-t (lower left), and fluorescence (lower right) from the 31 August – 4 October 2011 survey.

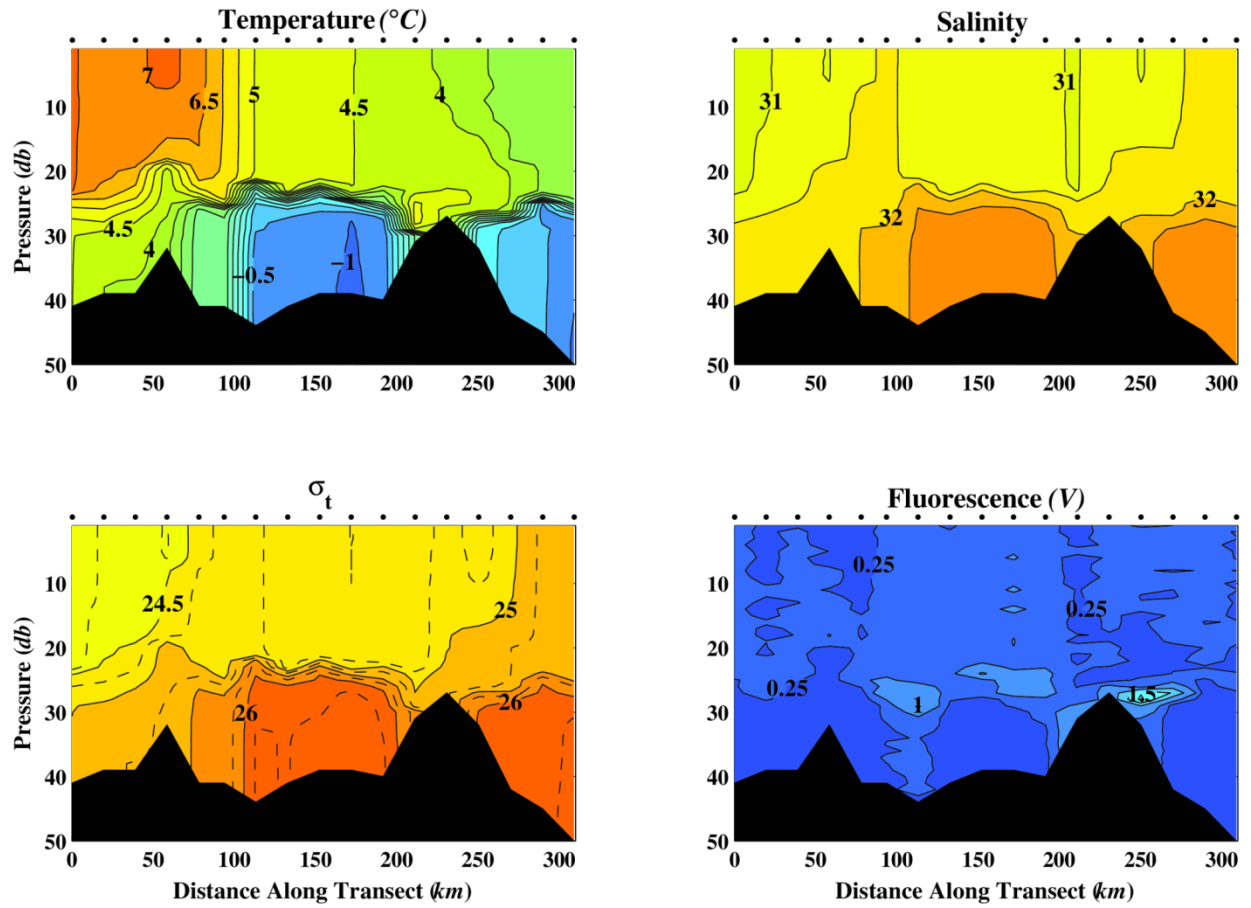

Figure 25. Southwest-northeast (SWNE3) section (per **Figure 13**) of temperature (upper left), salinity (upper right), sigma-t (lower left), and fluorescence (lower right) from the 31 August – 4 October 2011 survey.

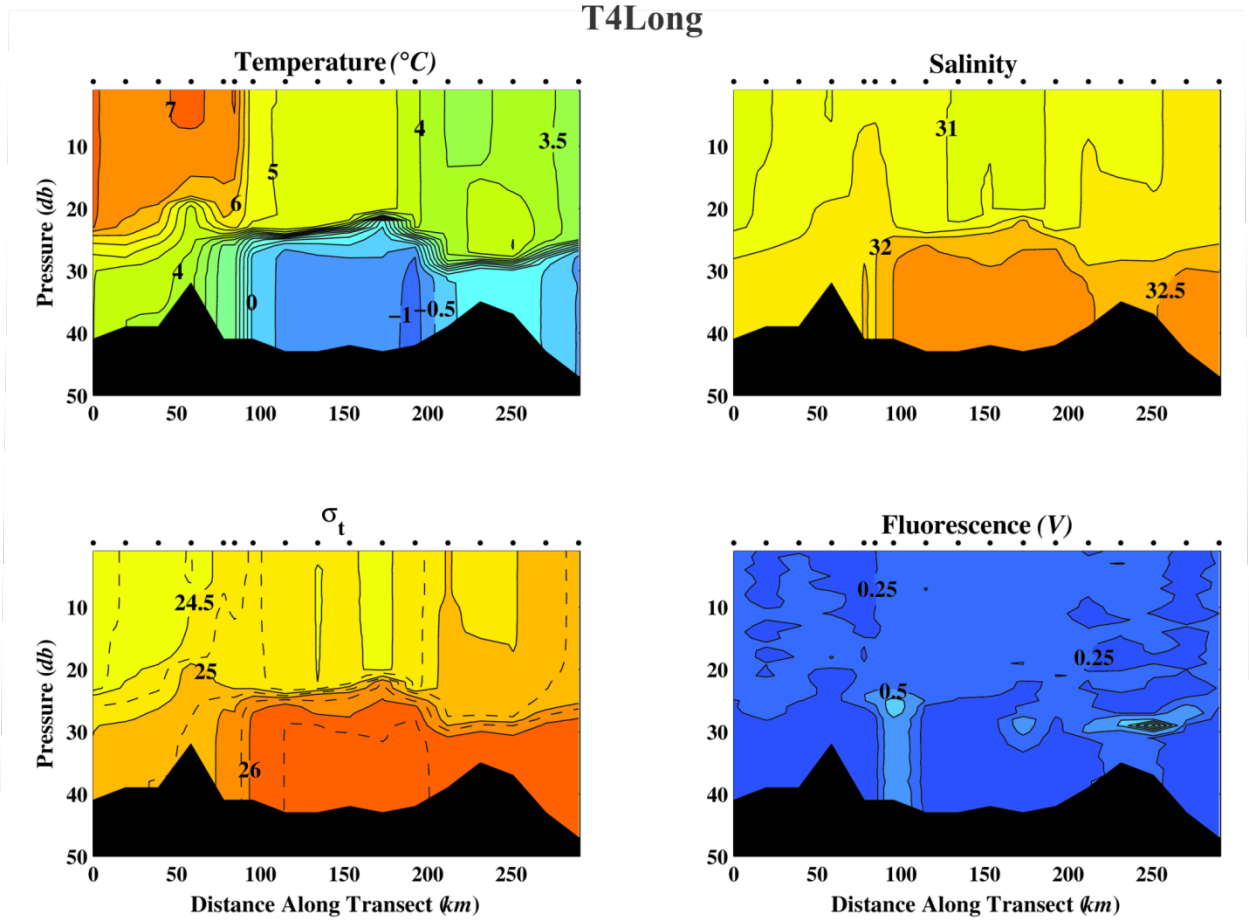

Figure 26. Southwest-northeast (T4long) section (per **Figure 13**) of temperature (upper left), salinity (upper right), sigma-t (lower left), and fluorescence (lower right) from the 31 August – 4 October 2011 survey.

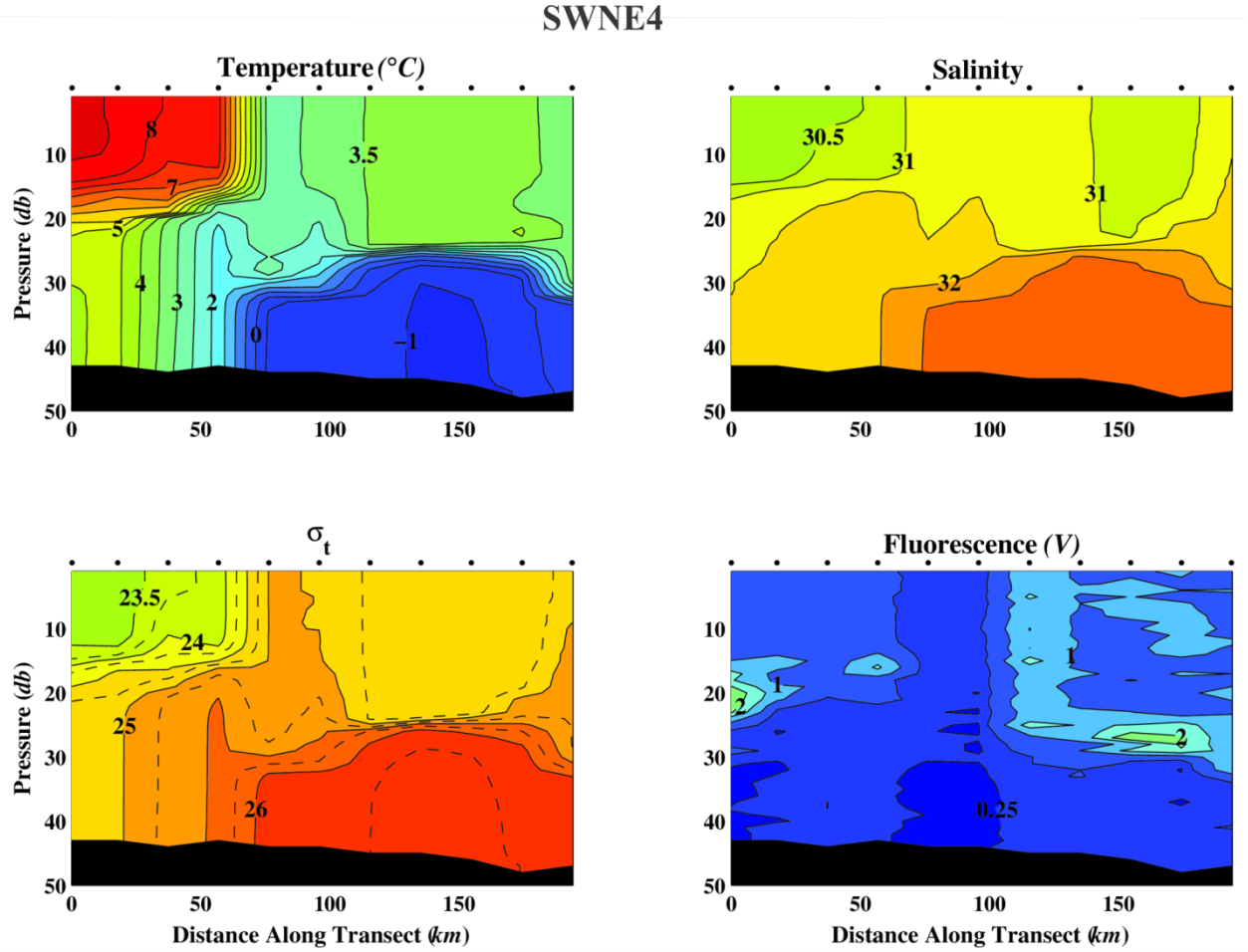

Figure 27. Southwest-northeast (SWNE3) section (per **Figure 13**) of temperature (upper left), salinity (upper right), sigma-t (lower left), and fluorescence (lower right) from the 31 August – 4 October 2011 survey.

We conclude this section by examining the horizontal distributions of temperature and salinity averaged below the mixed layer for both surveys (**Figure 28**). The maps clearly show that the cold, salty bottom waters observed in Statoil during the first cruise were replaced by warmer, less salty water while cold, dense water protruded southward and westward into Burger between the two cruises. The convergence of these opposing flows results in the formation of a strong thermal (and haline) front between the two regions. Moreover, the data suggest that warmer and fresher water moved northward into the area along the southern boundary of the broader survey area. These water masses have different densities, whose horizontal gradients will support a vertically-sheared geostrophic flow tendency. Assuming negligible bottom velocities, the geostrophic shear implies velocities (assuming that the bottom is at rest) of from 1 - 3 cm s^{-1} (and in the direction suggested by the arrows in the upper right panel of **Figure 28**). These speeds are much weaker than the measured flows (5 – 10 cm s^{-1}) in this region based on both current meter data (Weingartner et al., in review) and the vessel-mounted ADCP data discussed next.

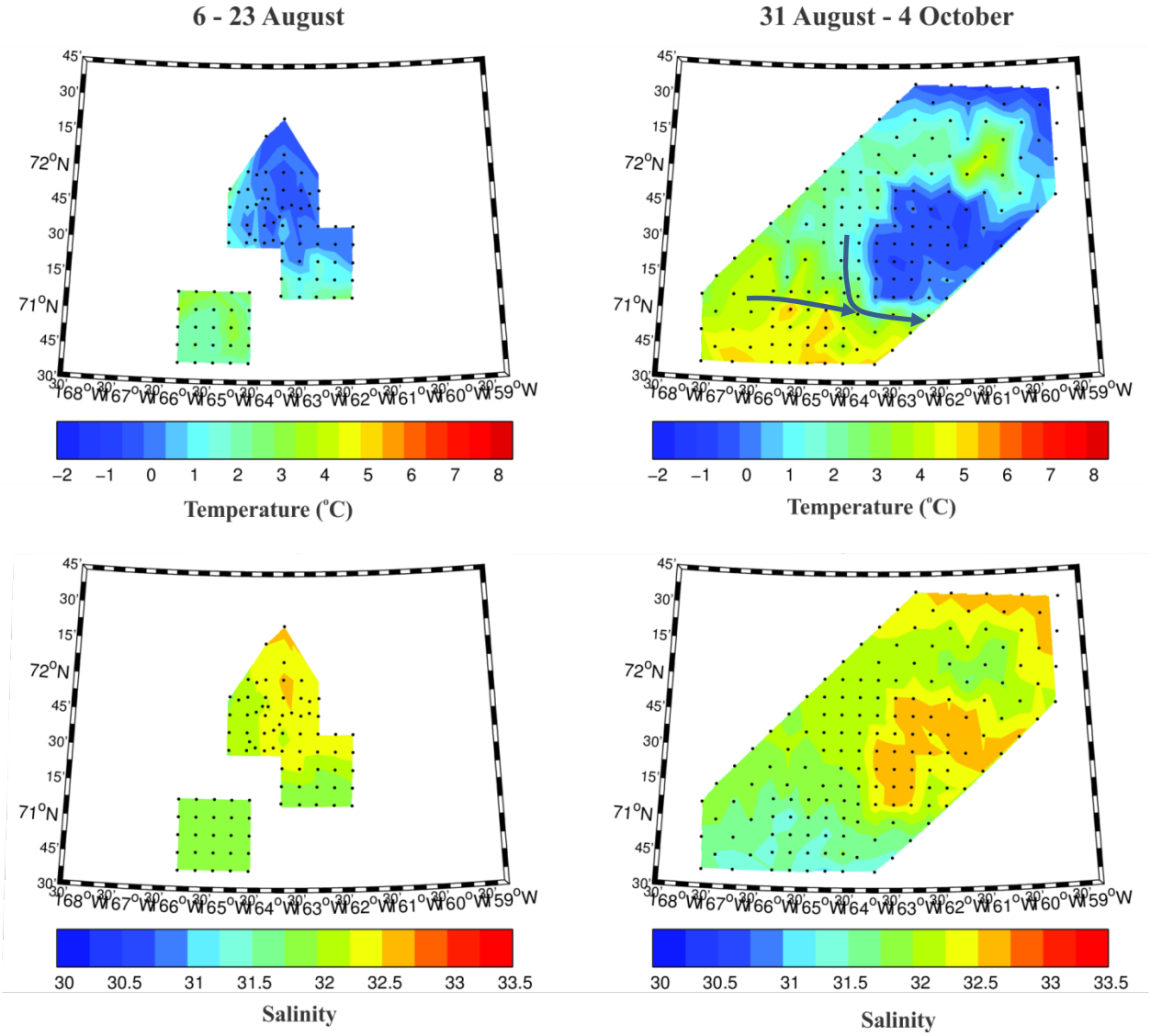

Figure 28. Contour maps of temperature and salinity bottom. Panels on the left are from the 6 – 23 August survey and those on the right are from the 31 August – 4 October 2011 survey.

A synoptic view of the circulation as captured by the vessel-mounted ADCP during the mooring deployment cruise of 28 July – 3 August 2011 at depths of 15, 21, and 31 m is shown in **Figure 29**. Several prominent features are evident in the figure:

1. The east-southeastward flow in Klondike and the southern half of Burger,
2. The strong onshore (eastward) flow to the east of Burger, which then
3. Veers northward into Barrow Canyon,
4. The northeastward flow west of Icy Cape that enters into Barrow Canyon,
5. The northwestward flow offshore flow west of Pt. Lay,
6. The southwestward flow along about 72°N and between 160° and 162°W,
7. And the comparatively weak and directionally variable flow between 71° 30'N and 72°N and 161° and 159°W, and,
8. The strong northeastward flow offshore of Barrow.

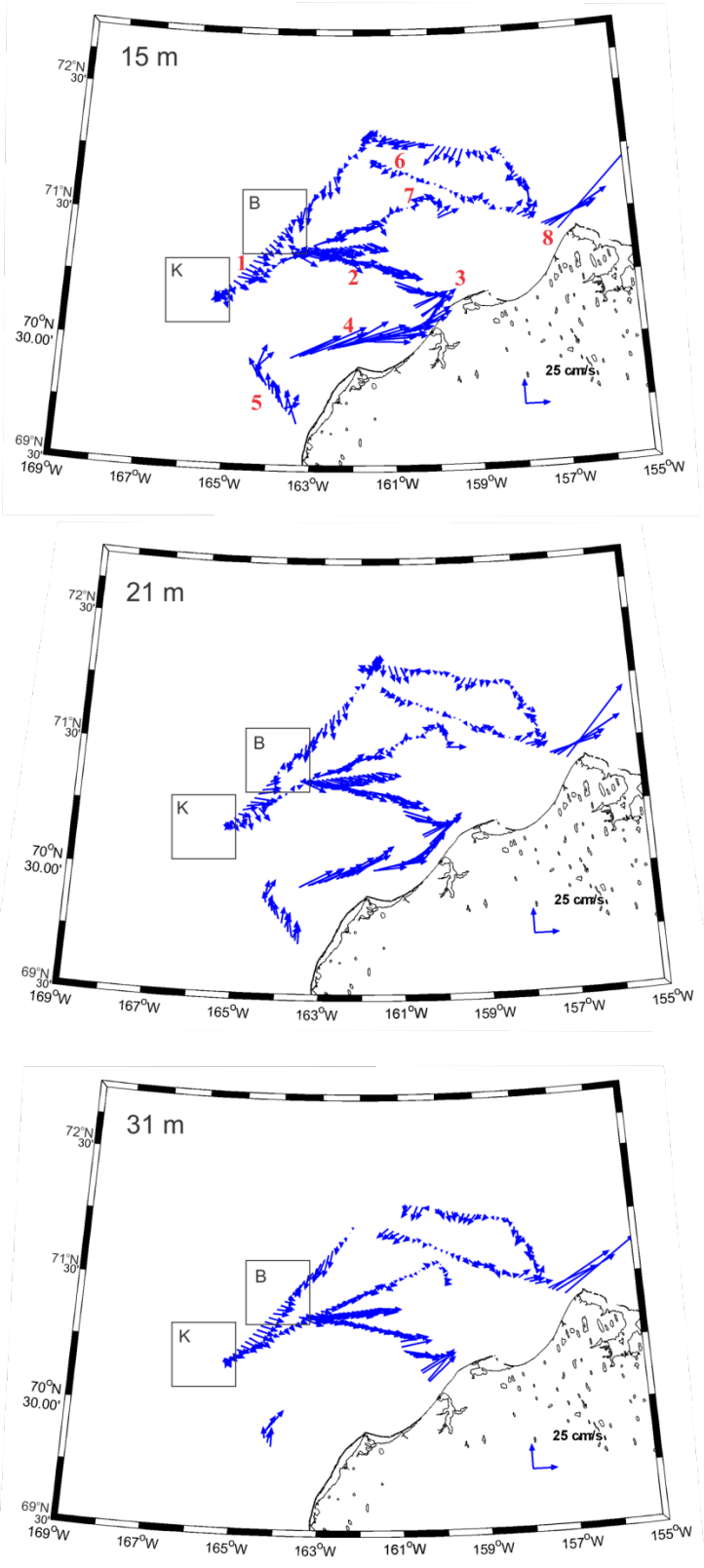

Figure 29. Velocity vectors at 15m (top), 21 m (middle), and 31 m (bottom) from the 28 July – 3 August 2011 mooring cruise. The letters K and B denote the locations of Burger and Klondike, respectively. The red numbers refer to specific circulation features elaborated upon in the text.

Note that in general, there is little difference in the velocities with depth, with the exception of region 6, where the currents veer and diminish in magnitude with depth.

Point 1 is consistent with the general seasonal transition in water properties in Klondike and Burger. This involves the eastward movement of warm, moderately salty Bering Sea Water in summer, which displaces cool, dilute surface meltwaters and cold, saline subsurface winter waters. Point 2 suggests that the eastward flow across the Klondike and southern Burger strengthens as it approaches the coast and then merges in Barrow Canyon (3) with warmer and fresher Alaskan Coastal Water moving to the northeast (4) offshore of Icy Cape. Point 6 suggests southwestward flow along the eastern side of Hanna Shoal that carries winter waters onto this portion of the shelf and, possibly, into the Burger area.

Many of the features seen in **Figure 29** are also evident in the mean surface current map (**Figure 30**) for August 2011 derived from shore-based high-frequency radars deployed in Barrow, Waintwright, and Pt. Lay (Weingartner et al., 2012). These include the offshore flow to the west of Pt. Lay (Point 5), the intensification of the eastward flow as it approaches Wainwright (Point 2) and merges with Alaskan Coastal Water (Point 4) in Barrow Canyon (Point 3).

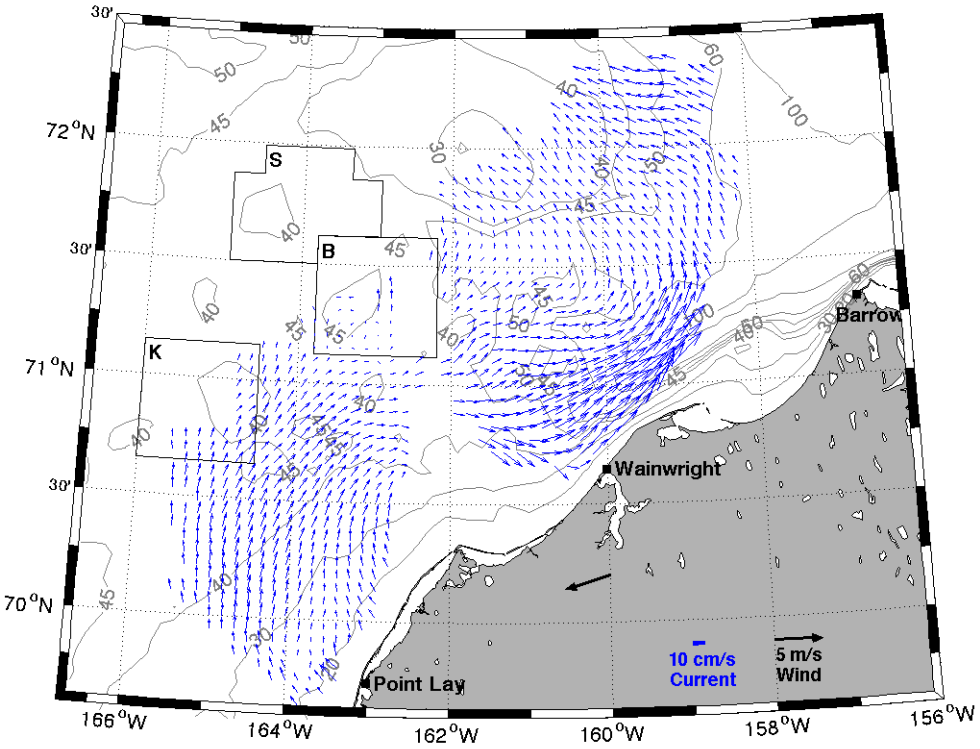

Figure 30. Mean August 2011 surface currents measured by High-Frequency Radars at Pt. Lay, Wainwright, and Barrow. The black vector over land indicates the mean August wind over the northeast Chukchi Sea.

Discussion and Conclusions

This preliminary analysis of the 2011 data set indicates that ice retreated earlier from the northeast Chukchi Sea shelf compared to the years 2008 – 2011. Conceivably this early retreat led to the virtual absence of meltwater in the study area during the surveys. As a consequence, stratification in August 2011 appeared weaker than in previous years. Moreover, August 2011 upper (~15 m) temperatures were also warmer than in previous years and surface horizontal temperature gradients were weak. While this may also be a consequence of the early ice retreat, the warmer temperatures might also reflect a greater heat flux through Bering Strait than in the other years.

The wind field from June through September 2011 was also quite different than in the previous years surveyed. While the mean winds were from the northeast on average, consistent with the other years, they were remarkably persistent from this direction and showed comparatively less variability in either magnitude or direction. Although the westward component of the winds appears to be effective in moving ice offshore of the coast in the northeast Chukchi Sea, we expected the southward wind component to advect ice onto the shelf. This clearly did not occur and suggests that broader scale-forcing is an important component of ice retreat over this portion of the shelf. On the other hand, the steadiness of the winds may have been quite effective in dispersing (via advection or vertical mixing) meltwaters from this region.

The results corroborate those reported by Weingartner et al. (in review) that advection over this portion of the shelf is a major component of the shelf heat budget. In particular we note that both Statoil and Klondike received major subsurface contributions of warm water between the two surveys, while the subsurface pool of cold water expanded and cooled between both cruises. As in 2010, it appears that the warming in Klondike and Statoil was due to advection from the east or south, while the cooling in Burger was due to a southwestward movement of cold, winter waters from the east of Hanna Shoal. These differential movements of subsurface waters resulted in rather strong horizontal temperature gradients, or fronts at depth. The eastward movement across Klondike and Statoil may, in part, be driven by the meridional density gradient in which ocean densities (particularly sub-surface) increase northward. From the thermal wind relationship, the baroclinic pressure gradient appears sufficient to sustain an ~2 cm s^{-1} eastward drift across the region south of Hanna Shoal.

The absence of meltwater in 2011 resulted in different patterns of stratification compared to the other years. Stratification was weaker in 2011 in Klondike and Statoil compared to previous years, and, in these study areas, the stratification was largely due to temperature. In previous years the major stratifiying agent was the vertical salinity gradient. In contrast, both temperature and salinity contributed to the vertical stratification in Burger. Moreover, the stratification in Burger was stronger than in either Klondike or Statoil.

As found in the other years, the chlorophyll distribution (reflected in fluorescence patterns) was patchy, with maximum values found slightly below the middle of the pycnocline, but overlying the coldest shelf waters. This suggests that nutrients in the surface waters and the inflowing Bering Sea Water were exhausted within the study area, while concentrations sufficient to support primary production existed within the winter waters.

Finally, we note that the circulation field measured by the vessel-mounted ADCP survey prior to the CTD surveys indicated eastward flow across Klondike and the southern half of Burger, with this flow then continuing eastward to enter Barrow Canyon. That survey also indicated southwestward flow along the east side of Hanna Shoal. That flow apparently transports winter water (along the bottom) into Burger. These opposing flow tendencies across Burger, if persistent, would explain the persistence of winter water at depth through much of the summer and fall within Burger. The eastward flow across Klondike (and presumably Statoil) is responsible for the advection of Bering Sea Water, which, on a seasonal basis replaces the winter water that resides in early summer in these areas.

References.

Coachman, L. K., Aagaard, K., Tripp, R.B., 1975. Bering Strait: The Regional Physical Oceanography, Univ. of Washington Press, Seattle, 172 pp.

Mesinger, F., and 19 Coauthors, 2006. North American regional re-analysis, *Bull. Amer. Meteor. Soc.*, 87, 343–360.

Pickart, R.S., Weingartner, T., Pratt, L.J., Zimmermann, S., Torres, D.J., 2005. Flow of winter-transformed Pacific water into the western Arctic. Deep-Sea Research, Part II 52: 3175 - 3198.

Shroyer, E. L., Plueddemann, A.J., Wind-driven modification of the Alaskan coastal current. Journal of Geophysical Research, accepted.

Spall, M. A., 2007. Circulation and water mass transformation in a model of the Chukchi Sea. Journal of Geophysical Research 112, C05025,doi:10.1029/2005JC002264.

Spreen, G., Kaleschke, L., Heygster, G., 2008. Sea ice remote sensing using AMSR-E 89 GHz channels. Journal of Geophysical Research 113, C02S03, doi:10.1029/2005JC003384.

Walsh, J.J., McRoy, C.P., Coachman, L.K., Goering, J.J., Nihoul, J.J., Whitledge, T.E., Blackburn, T. H., Parker, P.L., Wirick, C.D., Shuert, P.G., Grebmeier, J.M., Springer, A.M., Tripp, R.D., Hansell, D.A., Djenedi, S., Deleersnijder, S., Henriksen, K., Lund, B.A., Andersen, P., Müller-Karger, F.E., Dean, K., 1989. Carbon and nitrogen cycling within the Bering/Chukchi seas: Source regions for organic matter affecting AOU demands of the Arctic Ocean. Progress in Oceanography 22, 277-359.

Weingartner, T., E. Dobbins, S. Danielson, P. Winsor, R. Potter, and H. Statscewich. Hydrographic variability over the northeastern Chukchi Sea shelf in summer-fall 2008–2010. Continental Shelf Research (in review).

Weingartner, T., P. Winsor, R. Potter, , and H. Statscewich, and E. Dobbins. 2012. Application of High Frequency Radar to Potential Hydrocarbon Development Areas in the Northeast Chukchi Sea. *Draft Final Report to the* U.S. Department of the Interior Bureau of Ocean Energy Management, Alaska Outer Continental Shelf Region, ConocoPhillips, Inc., and

Shell Exploration & Production Company (Contract No: M09AC15207 as part of the BOEM Alaska Environmental Studies Program). 100p.

Weingartner, T., Aagaard, K., Woodgate, R., Danielson, S., Sasaki, Y., Cavalieri, D., 2005. Circulation on the North Central Chukchi Sea Shelf. Deep-Sea Research, Part II 52: 3150-3174, doi:10.1016/j.dsr2.2005.10.015.

Winsor, P., Chapman, D. C., 2004. Pathways of Pacific Water across the Chukchi Sea: A numerical model study. Journal of Geophysical Research 109, C03002, doi: 1029/2003JC001962.

Woodgate, R.A., Aagaard, K., Weingartner, T. J., 2005a. Monthly temperature, salinity, and transport variability of the Bering Strait through flow. Geophysical Research Letters 32, L04601, doi:10.1029/2004GL021880.

Woodgate, R. A., Aagaard, K., Weingartner, T. J., 2005b. A year in the physical oceanography of the Chukchi Sea: Moored measurements from autumn 1990-1991, Deep-Sea Research Part II, *52*(24-26), 3116-3149.